Three-dimensional Polarized Quark Distributions in the Nucleon

HENPIC Roundtable Discussions
May 8th, 2025

Tianbo Liu (刘天博)

Key Laboratory of Particle Physics and Particle Irradiation (MOE)
Institute of Frontier and Interdisciplinary Science, Shandong University
Southern Center for Nuclear-Science Theory, IMP, CAS

In collaboration with: Hongxin Dong, Bo-Qiang Ma, Peng Sun, Ke Yang, Chunhua Zeng, Yuxiang Zhao

山东大学
SHANDONG UNIVERSITY

SCNT
Southern Center for Nuclear-Science Theory

How much do we understand our world?

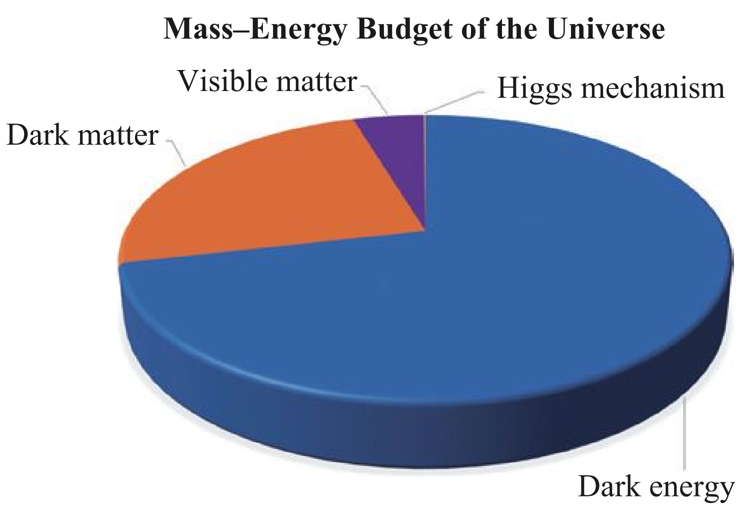

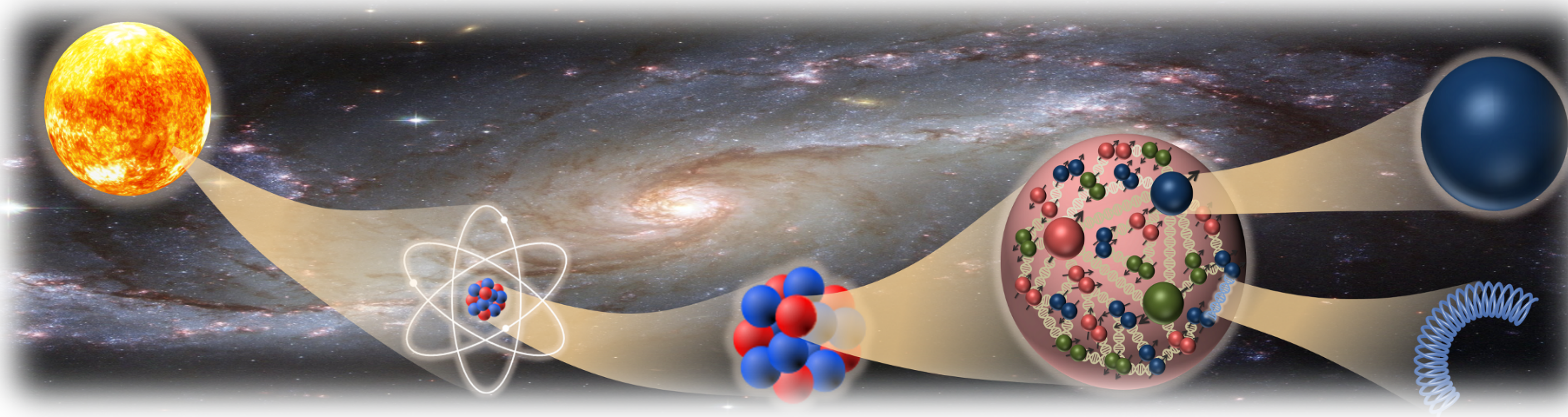

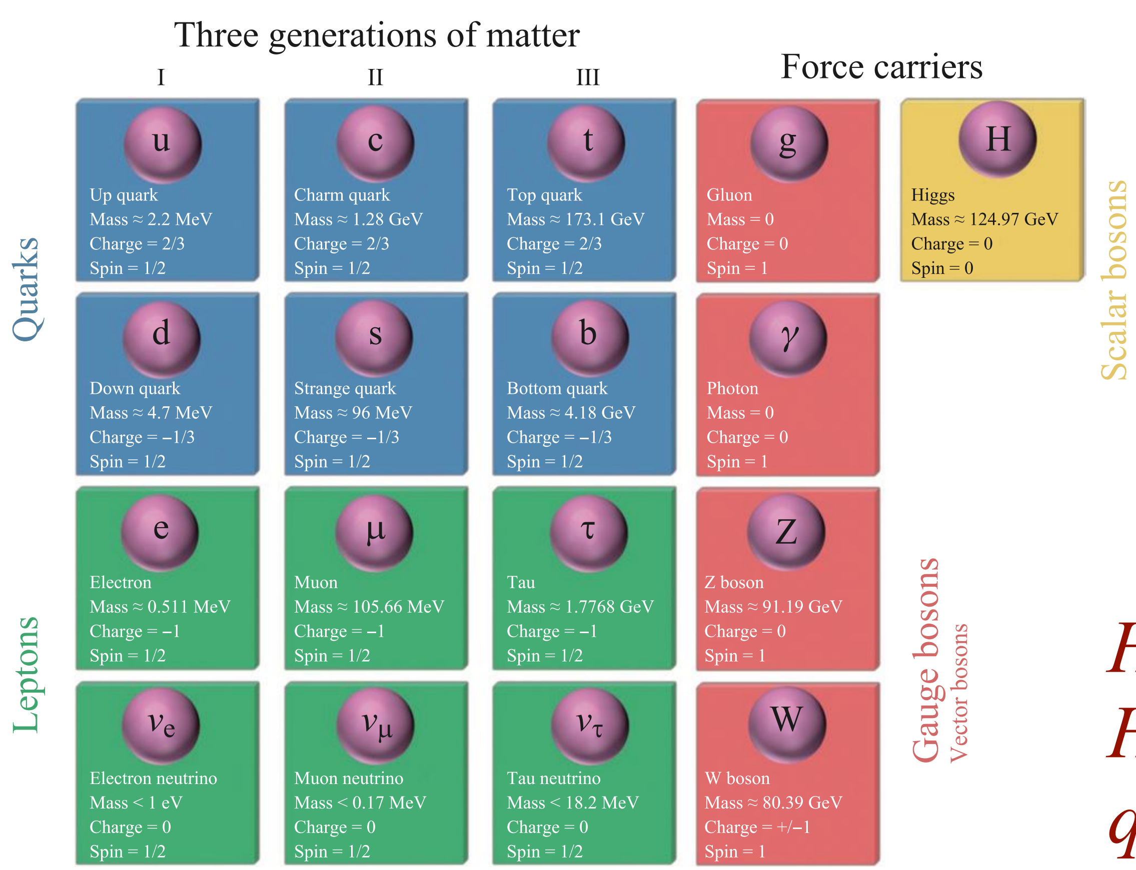

Mass

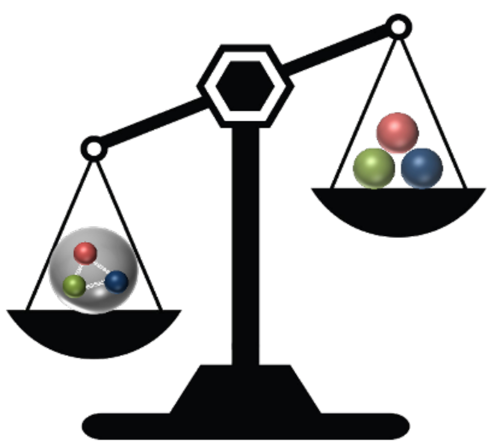

Spin

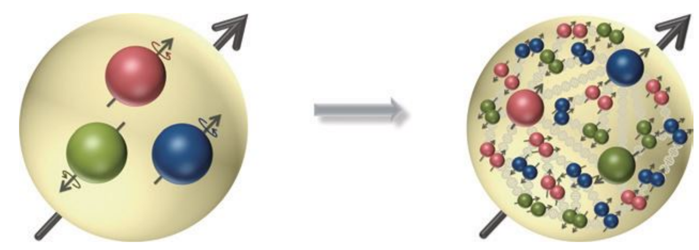

How do quarks and gluons make up a nucleon?
How can nucleon properties be explained at quarks and gluons degrees of freedom?

Proton Spin Structure in Naïve Quark Model

Quark model:

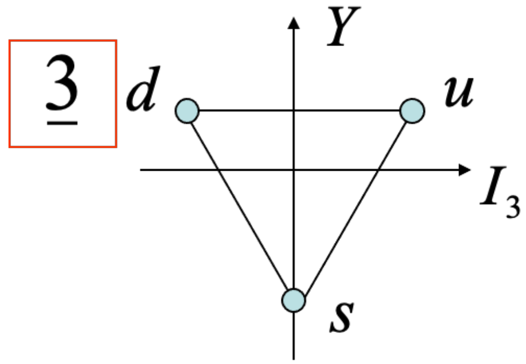

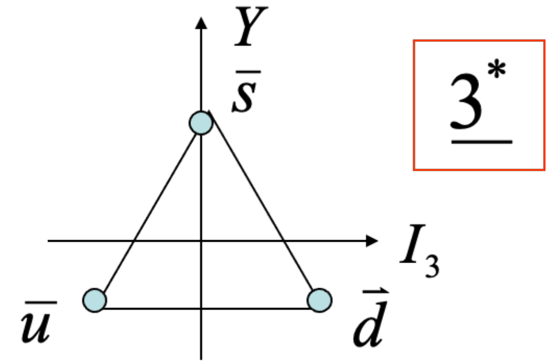

M. Gell-Mann, Phys. Lett. 8, 214 (1964);
G. Zweig, CERN Report No. TH-401 (1964).

ordinary baryons: $|qqq\rangle$, mesons: $|q\bar{q}\rangle$

Spin-flavor wave function of the proton:

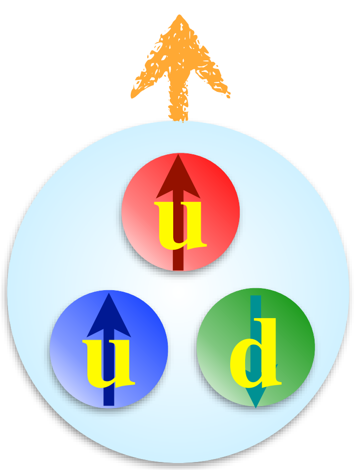

$$\left|p_\uparrow\right\rangle = \frac{1}{\sqrt{18}}\Big[2\left|u_\uparrow d_\downarrow u_\uparrow\right\rangle + 2\left|u_\uparrow u_\uparrow d_\downarrow\right\rangle + 2\left|d_\downarrow u_\uparrow u_\uparrow\right\rangle - \left|u_\uparrow u_\downarrow d_\uparrow\right\rangle$$
$$- \left|u_\uparrow d_\uparrow u_\downarrow\right\rangle - \left|u_\downarrow d_\uparrow u_\uparrow\right\rangle - \left|d_\uparrow u_\downarrow u_\uparrow\right\rangle - \left|d_\uparrow u_\uparrow u_\downarrow\right\rangle - \left|u_\downarrow u_\uparrow d_\uparrow\right\rangle\Big].$$

$$\Delta u = u_\uparrow - u_\downarrow = \frac{4}{3} \qquad \Delta d = d_\uparrow - d_\downarrow = -\frac{1}{3}$$

The sum of quark spins gives the proton spin.

Lepton-Hadron Deep Inelastic Scattering

Inclusive DIS at a large momentum transfer: $Q \gg \Lambda_{\mathrm{QCD}}$

Modern "Rutherford" experiment.

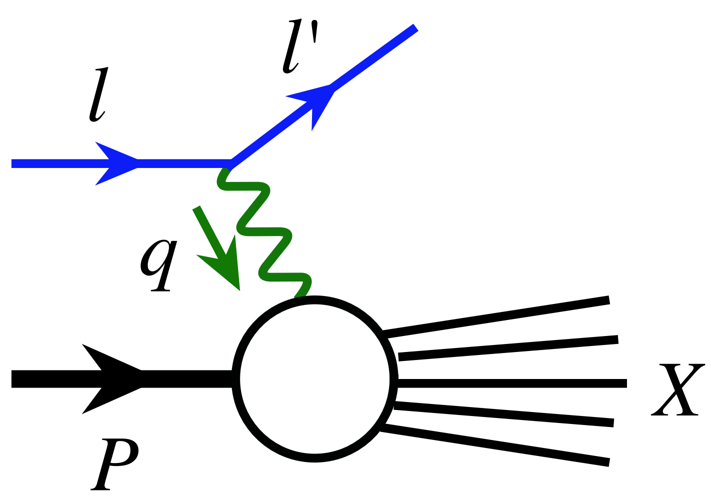

- dominated by the scattering of the lepton off an active quark/parton
- not sensitive to the dynamics at a hadronic scale ~ 1/fm
- collinear factorization:

$$\sigma \propto H(Q) \otimes f_{i/P}(x, \mu^2)$$

- overall corrections suppressed by $1/Q^n$
- indirectly "see" quarks, gluons and their dynamics
- predictive power relies on

— precision of the probe

— universality of $f_{i/P}(x, \mu^2)$

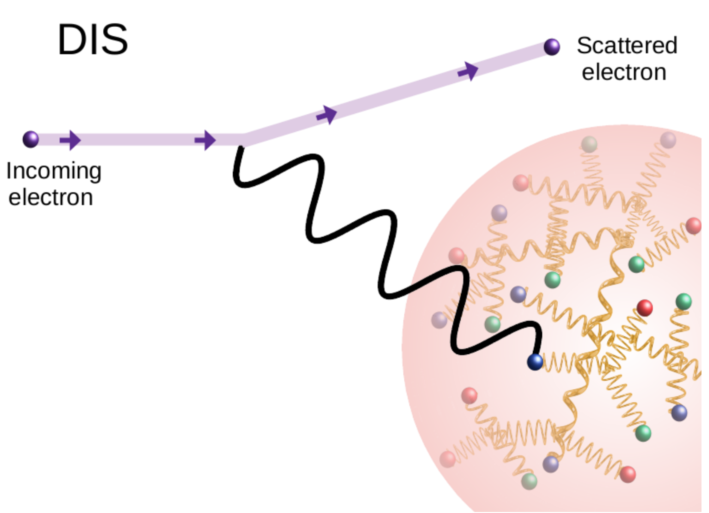

[Figure from DESY-21-099]

Lepton-Hadron Deep Inelastic Scattering

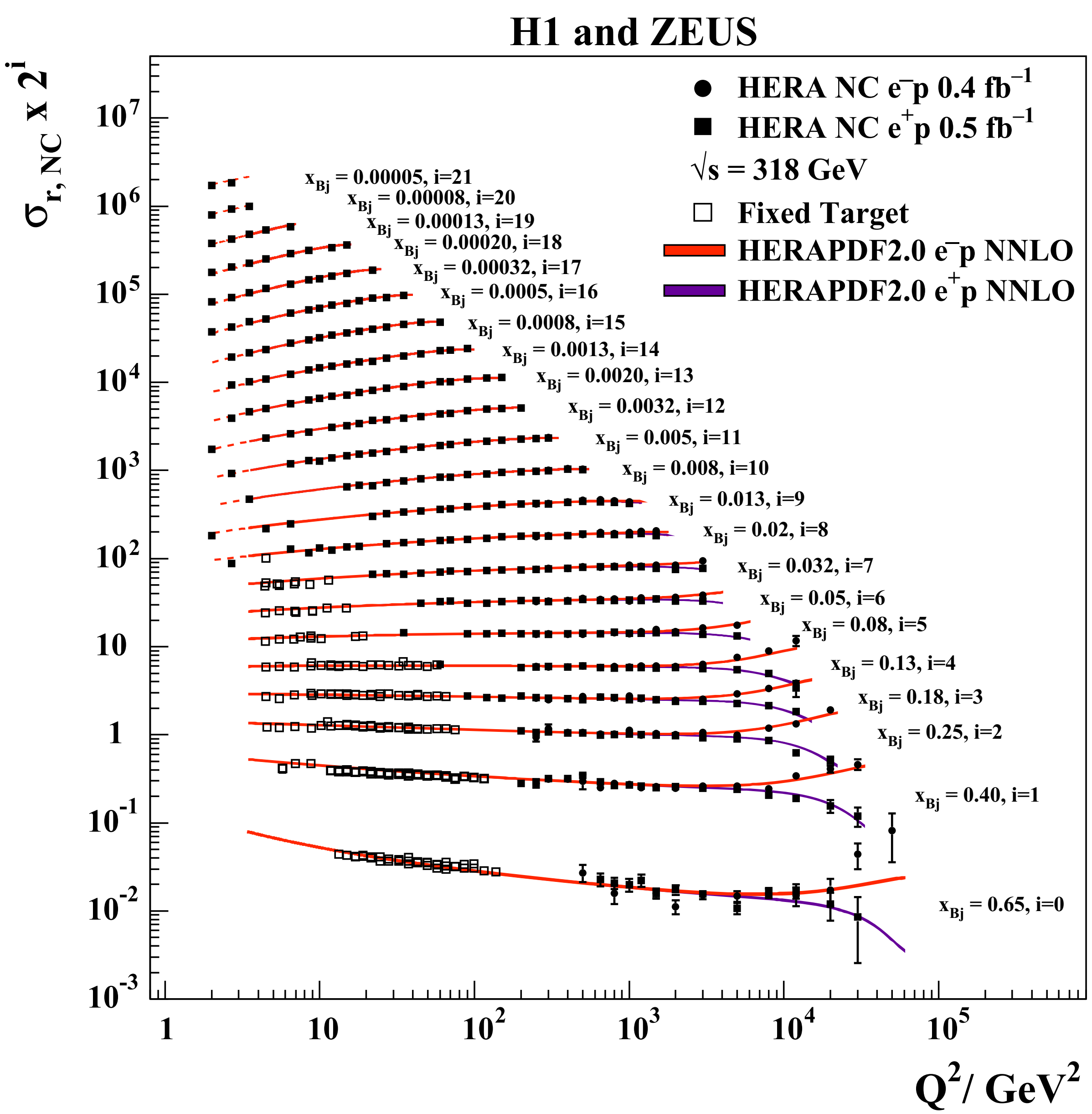

H. Abramowicz *et al.*, EPJC 78, 580 (2015).

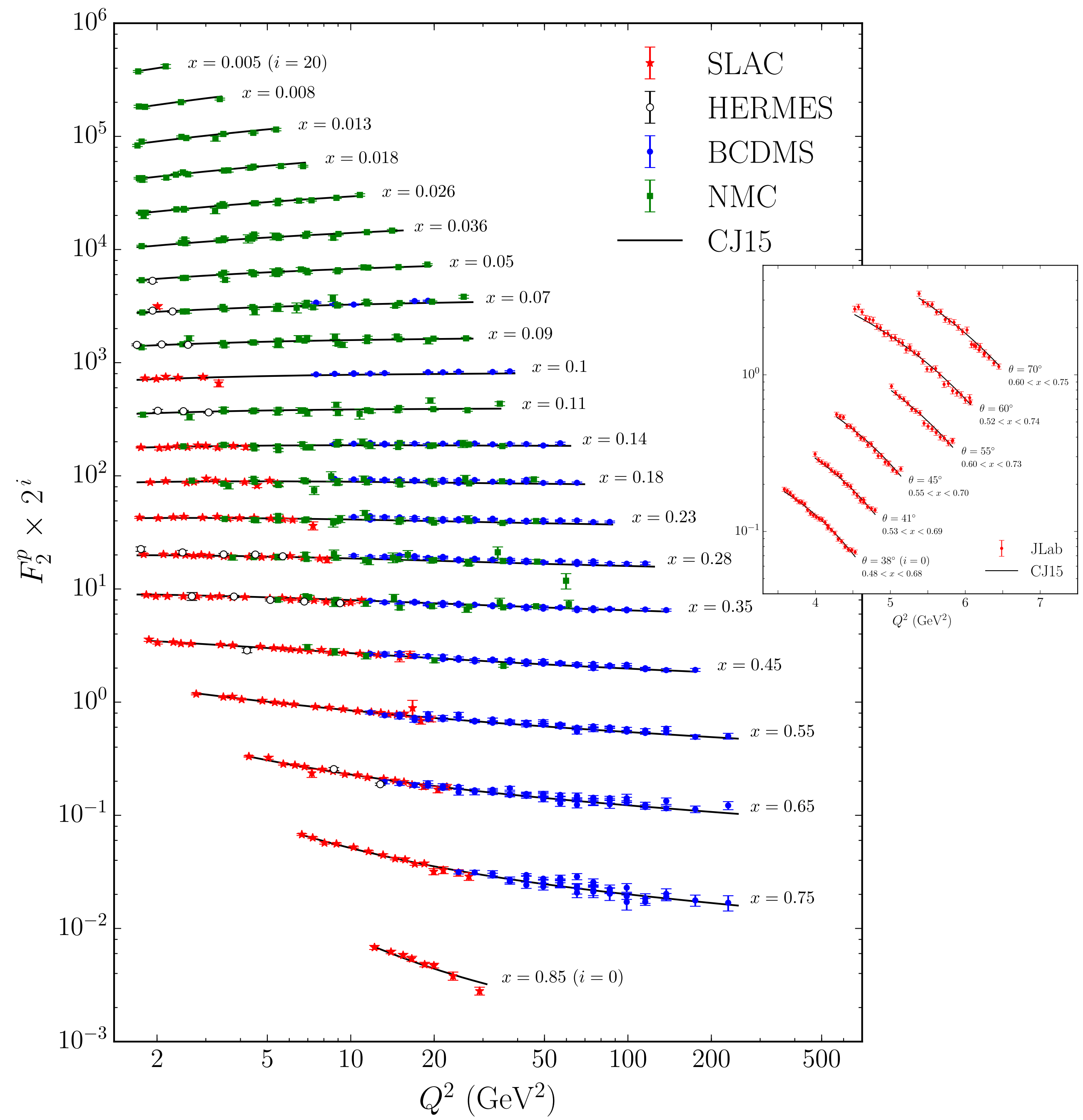

A. Accardi *et al.*, PRD 93, 114017 (2016).

Lepton-Hadron Deep Inelastic Scattering

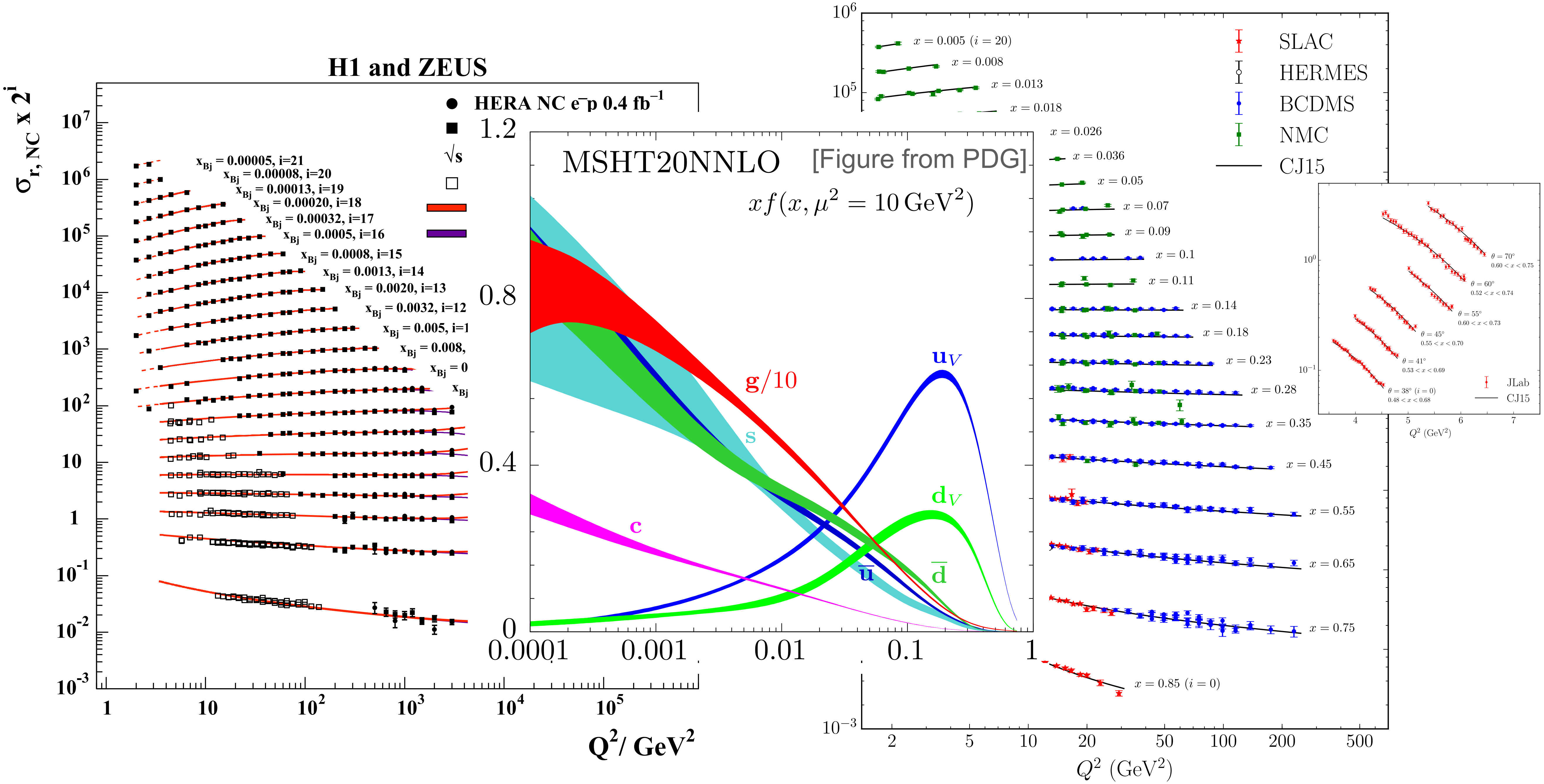

H. Abramowicz *et al.*, EPJC 78, 580 (2015).

A. Accardi *et al.*, PRD 93, 114017 (2016).

A successful story of QCD, factorization and evolution!

Nucleon Spin Structure

Proton spin puzzle

$$\Delta\Sigma = \Delta u + \Delta d + \Delta s \sim 0.3$$

Spin decomposition

$$J = \frac{1}{2}\Delta\Sigma + \Delta G + L_q + L_g$$

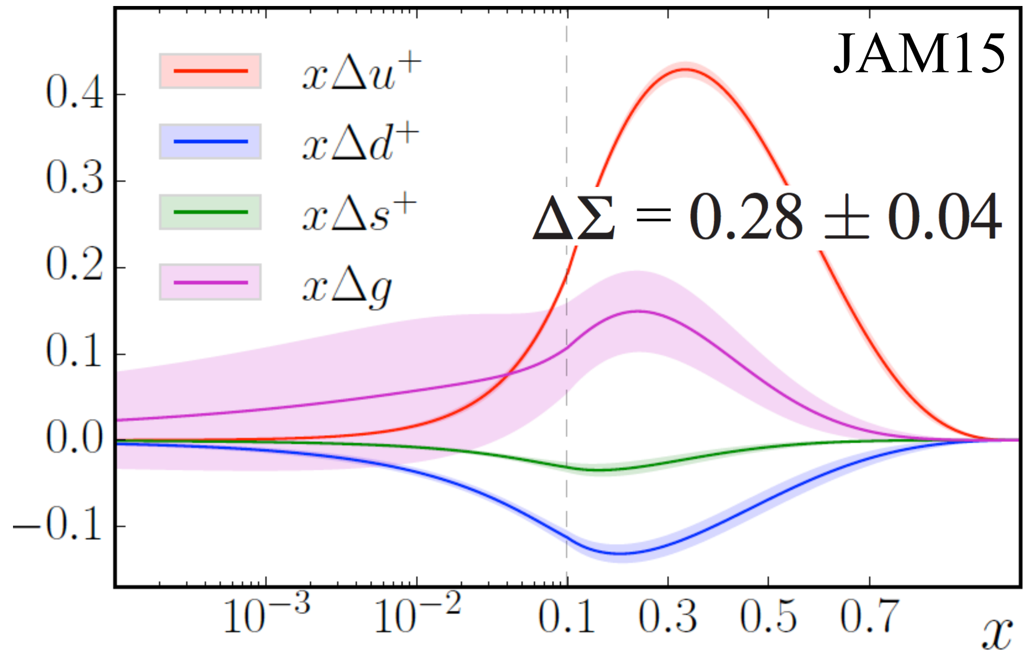

JAM Collaboration, PR D 93, 074005 (2016).

JAM17: $\Delta\Sigma = 0.36 \pm 0.09$

JAM Collaboration, PRL 119, 132001 (2017).

Quark spin only contributes a small fraction to the nucleon spin.

J. Ashman *et al.*, PLB 206, 364 (1988); NP B328, 1 (1989).

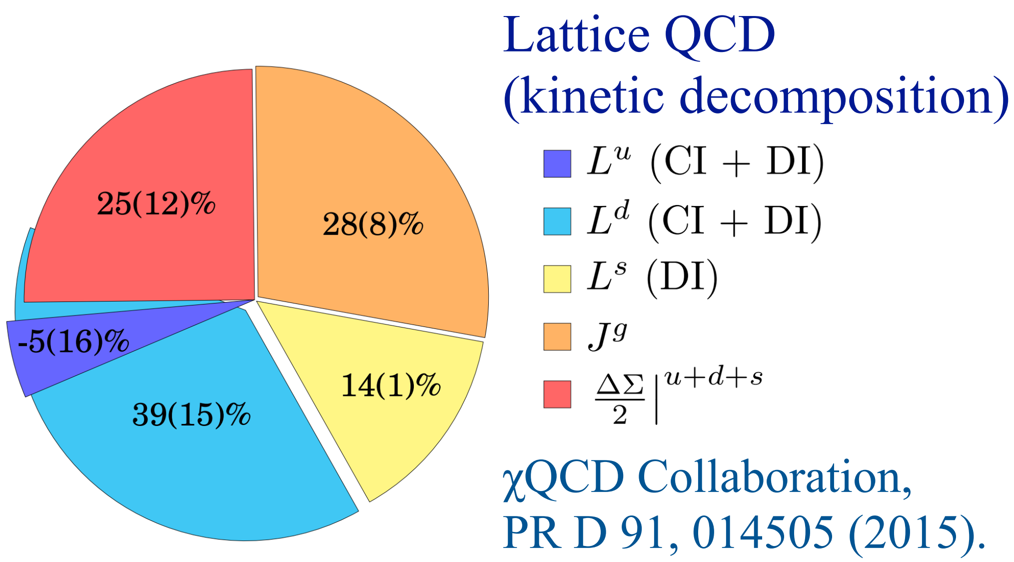

χQCD Collaboration, PR D 91, 014505 (2015).

Gluon spin from LQCD: $S_g = 0.251(47)(16)$

50% of total proton spin

Y.-B. Yang *et al.* (χQCD Collaboration), PRL 118, 102001 (2017).

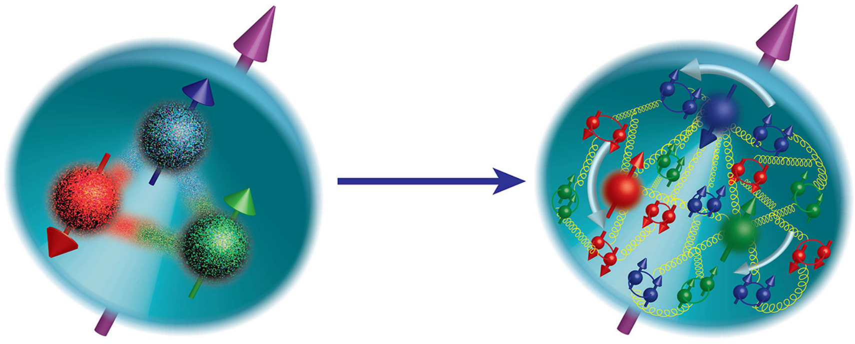

Wigner Rotation Effect

Melosh-Wigner rotation

quark spin in a rest proton $\neq$ quark spin in a moving proton

If applying a *kinetic boost*, one may relate the spin states in *proton rest frame* to the spin states in *infinite momentum frame*

$$\chi_T^{\uparrow} = w\left[\left(k^+ + m\right)\chi_F^{\uparrow} - \left(k^1 + ik^2\right)\chi_F^{\downarrow}\right]$$

$$\chi_T^{\downarrow} = w\left[\left(k^+ + m\right)\chi_F^{\downarrow} + \left(k^1 - ik^2\right)\chi_F^{\uparrow}\right]$$

$$k^+ = k^0 + k^3$$

$$w = \left[2k^+\left(k^0 + m\right)\right]^{-1/2}$$

E.P. Wigner, Ann. Math 40 (1939) 149; H.J. Melosh, Phys. Rev. D 9 (1974) 1095.

The effect on quark polarization

$$\Delta q = \int \mathrm{d}^3\mathbf{k}\,\mathscr{M}\left[q^{\uparrow}(k) - q^{\downarrow}(k)\right]$$

$$\mathscr{M} = \frac{(k^+ + m)^2 - k_T^2}{2k^+(k^0 + m)}$$

B.-Q. Ma, J. Phys. G 17 (1991) L53-L58; B.-Q. Ma, Q.-R. Zhang, Z. Phys. C 58 (1993) 479.

It predicts decreasing polarization with k_T, which should be tested by data.
This interpretation is based on a kinetic boost, but a complete boost including QCD dynamics is challenging.

Semi-inclusive Deep Inelastic Scattering

Semi-inclusive DIS: a final state hadron (P_h) is identified

- enable us to explore the emergence of color neutral hadrons from colored quarks/gluons
- flavor dependence by selecting different types of observed hadrons: pions, kaons, …
- a large momentum transfer Q provides a short-distance probe
- an additional and adjustable momentum scale P_{hT}
- multidimensional imaging of the nucleon

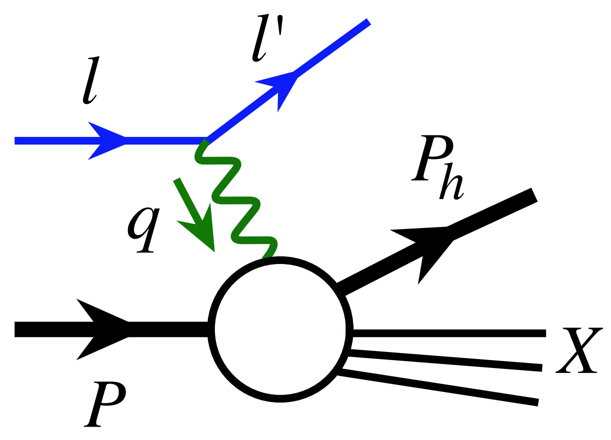

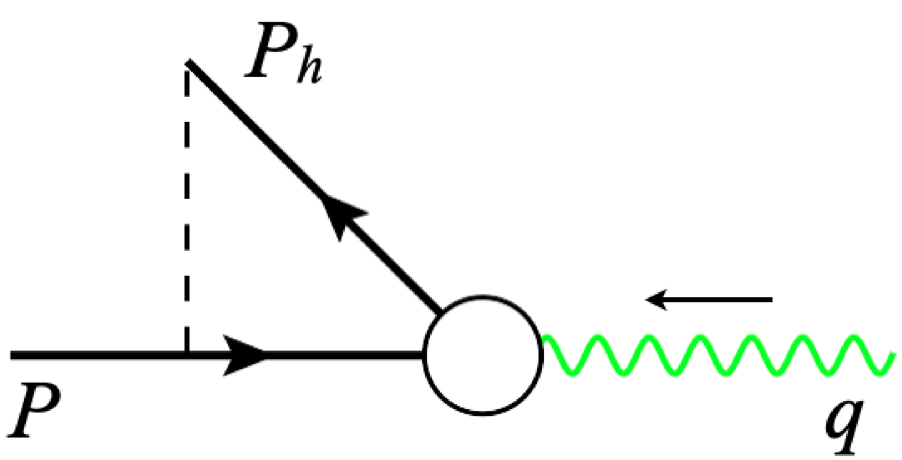

SIDIS Kinematic Regions

Sketch of kinematic regions of the produced hadron

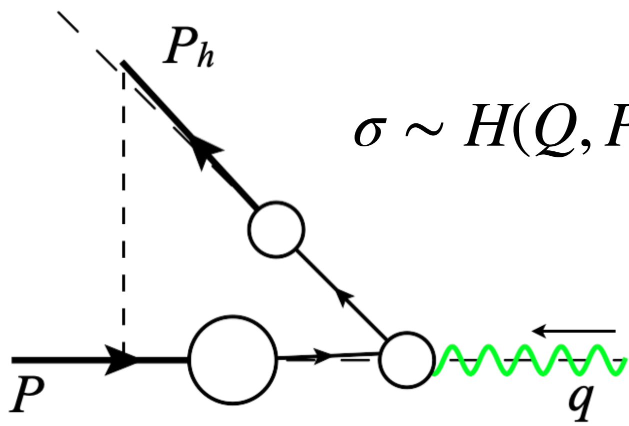

$$\sigma \sim H(Q, P_{hT}) \otimes f_{i/P}(x) \otimes D_{j\to h}(z)$$

$P_{hT} \sim Q$

$P_{hT} \ll Q$

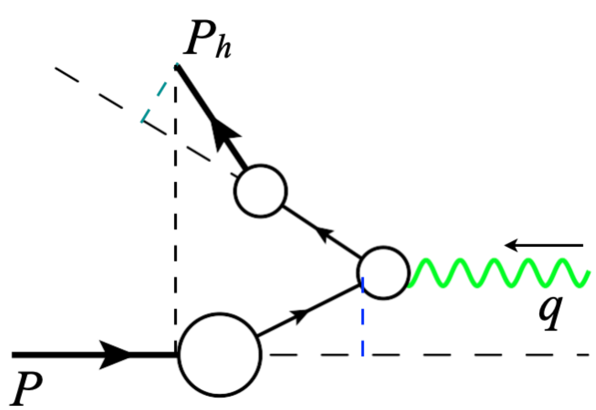

$$\sigma \sim H(Q) \otimes f_{i/P}(x, k_T) \otimes D_{j\to h}(z, p_T)$$

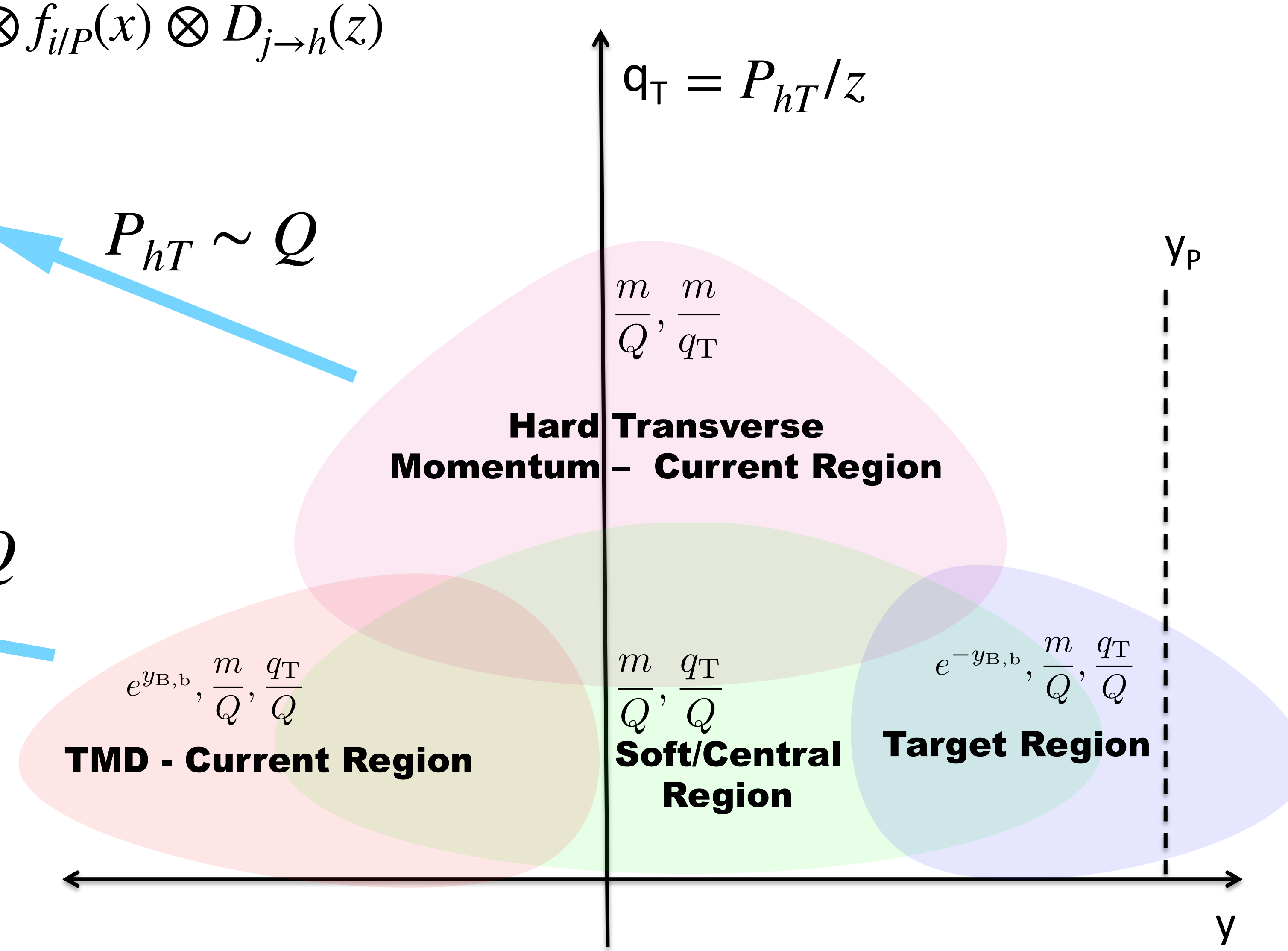

P_{hT} is defined in the photon-hadron frame

[Figure from JHEP10(2019)122]

Structure Functions of SIDIS

SIDIS differential cross section

in terms of 18 structure functions

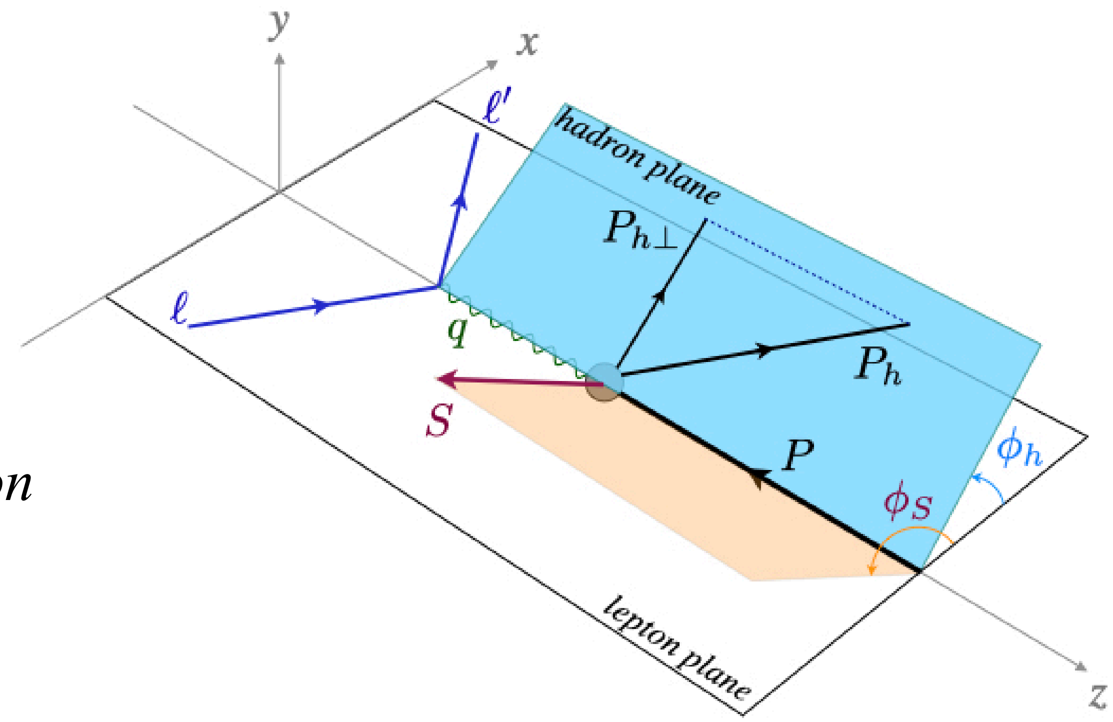

$$F_{AB,C}(x_B, z, P_{hT}^2, Q^2)$$

A: lepton polarization
B: nucleon polarization
C: virtual photon polarization

$$\frac{d\sigma}{dx_B\, dy\, dz\, dP_{hT}^2\, d\phi_h\, d\phi_S} = \frac{\alpha^2}{x_B y Q^2}\frac{y^2}{2(1-\epsilon)}\left(1+\frac{\gamma^2}{2x_B}\right)$$

$$\times \Big\{ F_{UU,T} + \epsilon F_{UU,L} + \sqrt{2\epsilon(1+\epsilon)}F_{UU}^{\cos\phi_h}\cos\phi_h + \epsilon F_{UU}^{\cos 2\phi_h}\cos 2\phi_h + \lambda_e\sqrt{2\epsilon(1-\epsilon)}F_{LU}^{\sin\phi_h}\sin\phi_h$$

$$+ S_L\left[\sqrt{2\epsilon(1+\epsilon)}F_{UL}^{\sin\phi_h}\sin\phi_h + \epsilon F_{UL}^{\sin 2\phi_h}\sin 2\phi_h\right] + \lambda_e S_L\left[\sqrt{1-\epsilon^2}F_{LL} + \sqrt{2\epsilon(1-\epsilon)}F_{LL}^{\cos\phi_h}\cos\phi_h\right]$$

$$+ S_T\Big[\left(F_{UT,T}^{\sin(\phi_h-\phi_S)} + \epsilon F_{UT,L}^{\sin(\phi_h-\phi_S)}\right)\sin(\phi_h-\phi_S) + \epsilon F_{UT}^{\sin(\phi_h+\phi_S)}\sin(\phi_h+\phi_S)$$

$$+ \epsilon F_{UT}^{\sin(3\phi_h-\phi_S)}\sin(3\phi_h-\phi_S) + \sqrt{2\epsilon(1+\epsilon)}F_{UT}^{\sin\phi_S}\sin\phi_S + \sqrt{2\epsilon(1+\epsilon)}F_{UT}^{\sin(2\phi_h-\phi_S)}\sin(2\phi_h-\phi_S)\Big]$$

$$+ \lambda_e S_T\Big[\sqrt{1-\epsilon^2}F_{LT}^{\cos(\phi_h-\phi_S)}\cos(\phi_h-\phi_S)$$

$$+ \sqrt{2\epsilon(1-\epsilon)}F_{LT}^{\cos\phi_S}\cos\phi_S + \sqrt{2\epsilon(1-\epsilon)}F_{LT}^{\cos(2\phi_h-\phi_S)}\cos(2\phi_h-\phi_S)\Big]\Big\}$$

$$x_B = \frac{Q^2}{2P\cdot q}$$

$$y = \frac{P\cdot q}{P\cdot l}$$

$$z = \frac{P\cdot P_h}{P\cdot q}$$

$$\gamma = \frac{2x_B M}{Q}$$

$$\epsilon = \frac{1-y-\frac{1}{4}\gamma^2y^2}{1-y+\frac{1}{2}y^2+\frac{1}{4}\gamma^2y^2}$$

Leading Twist TMDs

Nucleon Polarization	Quark Polarization: U	Quark Polarization: L	Quark Polarization: T
U	f_1 unpolarized		$h_1^{\perp}$ Boer-Mulders
L		g_{1L} helicity	$h_{1L}^{\perp}$ longi-transversity (worm-gear)
T	$f_{1T}^{\perp}$ Sivers	g_{1T} trans-helicity (worm-gear)	h_1 transversity $h_{1T}^{\perp}$ pretzelosity

Leading Twist TMDs

Nucleon Polarization	Quark Polarization: U	Quark Polarization: L	Quark Polarization: T
U	f_1 unpolarized		$h_1^{\perp}$ Boer-Mulders
L		g_{1L} helicity	$h_{1L}^{\perp}$ longi-transversity (worm-gear)
T	$f_{1T}^{\perp}$ Sivers	g_{1T} trans-helicity (worm-gear)	h_1 transversity $h_{1T}^{\perp}$ pretzelosity

Longitudinal Double Spin Asymmetry

Longitudinal DSA in SIDIS

$$A_{LL} \equiv \frac{\sigma_{++} - \sigma_{+-} + \sigma_{--} - \sigma_{-+}}{\sigma_{++} + \sigma_{+-} + \sigma_{--} + \sigma_{-+}} = \frac{\sqrt{1-\varepsilon^2} F_{LL}\left(x, z, P_{hT}^2, Q^2\right)}{F_{UU}\left(x, z, P_{hT}^2, Q^2\right)}$$

In TMD region:

$$F_{LL}\left(x, z, P_{hT}^2, Q^2\right) \sim g_{1L}(x, k_T^2) \otimes D_1(z, p_T^2)$$

$$F_{UU}\left(x, z, P_{hT}^2, Q^2\right) \sim f_1(x, k_T^2) \otimes D_1(z, p_T^2)$$

g_{1L} 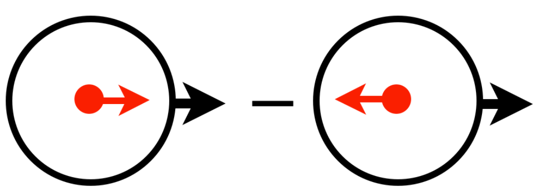

(both collinear and TMD)

One needs P_{hT}-dependent DSA measurements to determine TMD helicity distributions.

P_{hT} dependent DSA measurements

HERMES: proton (H_2) and deuteron (D_2) targets

HERMES Collaboration, Phys. Rev. D 99 (2019) 112001.

JLab CLAS: proton (NH_3) target

CLAS Collaboration, Phys. Lett. B 782 (2018) 662.

TMD Evolution

Evolution equations

$$\mu^2 \frac{dF(x,b;\mu^2,\zeta)}{d\mu^2} = \frac{\gamma_F(\mu,\zeta)}{2} F(x,b;\mu^2,\zeta)$$

$$\zeta \frac{dF(x,b;\mu^2,\zeta)}{d\zeta} = -\mathscr{D}(\mu,b) F(x,b;\mu^2,\zeta)$$

$$-\zeta \frac{d\gamma_F(\mu,\zeta)}{d\zeta} = \mu \frac{d\mathscr{D}(\mu,b)}{d\mu} = \Gamma_{\text{cusp}}(\mu)$$

$$\gamma_F(\mu,\zeta) = \Gamma_{\text{cusp}}(\mu) \ln \frac{\mu^2}{\zeta} - \gamma_V(\mu)$$

$$F\left(x,b;\mu_f,\zeta_f\right) = \exp\left[\int_P \left(\gamma_F(\mu,\zeta)\frac{d\mu}{\mu} - \mathscr{D}(\mu,b)\frac{d\zeta}{\zeta}\right)\right] F\left(x,b;\mu_i,\zeta_i\right)$$

ζ-prescription

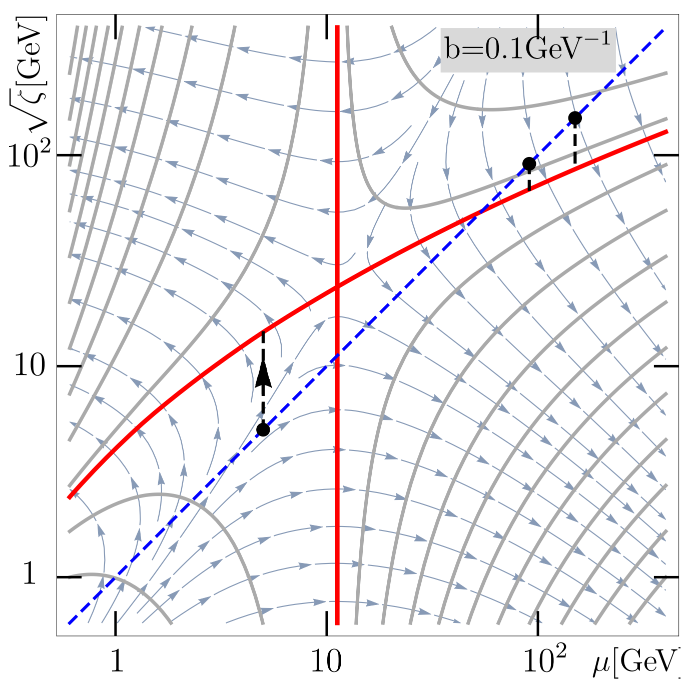

equipotential lines:

$$\frac{d \ln \zeta_\mu(\mu,b)}{d \ln \mu^2} = \frac{\gamma_F\left(\mu,\zeta_\mu(\mu,b)\right)}{2\mathscr{D}(\mu,b)}$$

$$\mathscr{D}\left(\mu_0,b\right) = 0, \quad \gamma_F\left(\mu_0,\zeta_\mu\left(\mu_0,b\right)\right) = 0$$

$$F\left(x,b;Q,Q^2\right) = \left(\frac{Q^2}{\zeta_Q(b)}\right)^{-\mathscr{D}(Q,b)} F(x,b), \quad \mu_f^2 = \zeta_f = Q^2$$

Parametrization

Parametrization of TMD helicity distributions

we parametrize the distributions in b space at the saddle point

$$g_{1L}(x,b) = \sum_{f'} \int_x^1 \frac{d\xi}{\xi} \Delta C_{f\leftarrow f'}\left(\xi, b, \mu_{\rm OPE}\right) g_{1L}^{f'}\left(\frac{x}{\xi}\right) g_{\rm NP}(x,b),$$

$$g_{1L}^f(x) = N_f \frac{(1-x)^{\alpha_f} x^{\beta_f}\left(1+\epsilon_f x\right)}{n\left(\alpha_f, \beta_f, \epsilon_f\right)} g_1^f\left(x, \mu_{\rm OPE}\right)$$

$n\left(\alpha_f, \beta_f, \epsilon_f\right)$ is introduced to reduce the correlation between normalization and the shape.

$$g_{\rm NP}(x,b) = \exp\left[-\frac{\lambda_1(1-x)+\lambda_2 x+\lambda_5 x(1-x)}{\sqrt{1+\lambda_3 x^{\lambda_4} b^2}} b^2\right]$$

the same form as adopted in the unpolarized distributions.

The x-dependent factor allows a variation from the collinear distribution.
Such an x-shape modification can be removed by setting $\alpha_f = \beta_f = \epsilon_f = 0$.

First Extraction of TMD Helicity

NLO+NNLL analysis results

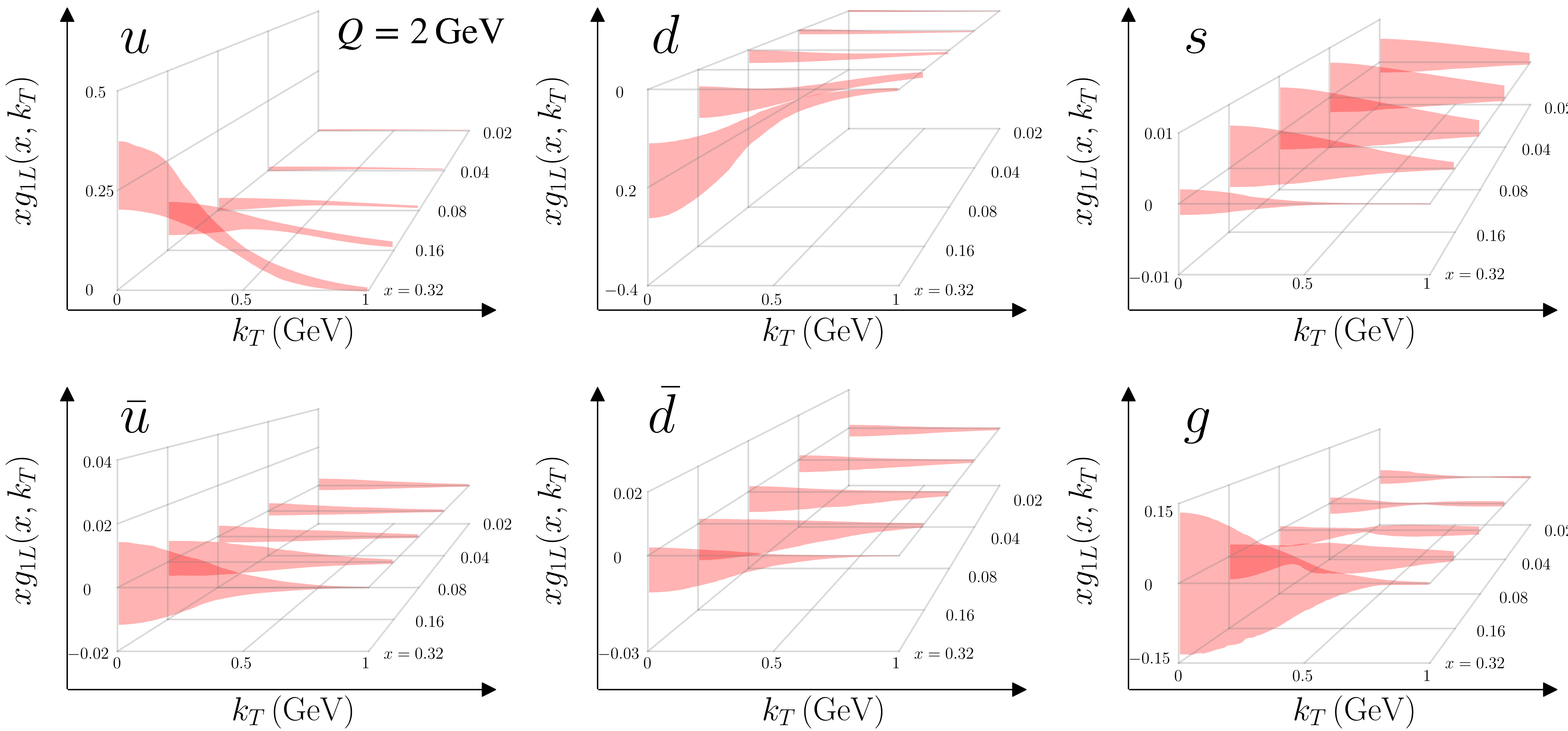

Nonzero signals for *u* and *d* quarks, while sea quarks and gluons are loosely constrained.

K. Yang, TL, P. Sun, Y. Zhao, B.-Q. Ma, Phys. Rev. Lett. 134 (2025) 121902.

Estimation of Uncertainties

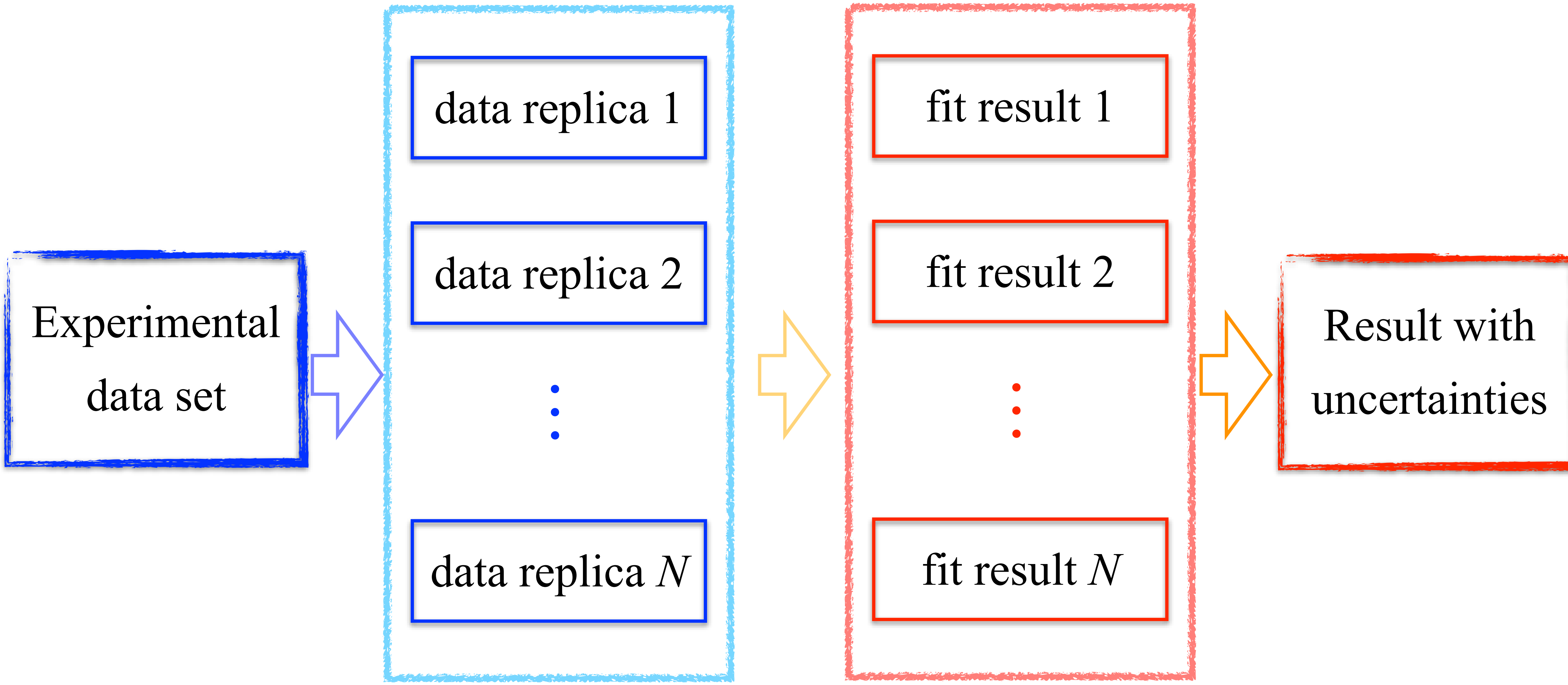

Monte Carlo representation of data distribution

Probability density in function space

Estimation of Uncertainties

In each single fit:

$$\text{minimize} \qquad \chi^2 = \sum_{\text{sets}} \sum_{i,j} (t_i - a_i)\, V_{ij}^{-1} \left(t_j - a_j\right) \qquad V_{ij} : \text{covariant matrix}$$

Dominant correlated uncertainties:

Experiment	Process	Beam and target polarization	Dilution
HERMES	$e^{\pm}p \to e^{\pm}hX$	6.6%	0
HERMES	$e^{\pm}d \to e^{\pm}hX$	5.7%	1.7%
CLAS	$e^{-}p \to e^{-}\pi^{0}X$	4.5%	5.8%

In this study, 1000 replicas are generated according to data uncertainties and their correlations.

K. Yang, TL, P. Sun, Y. Zhao, B.-Q. Ma, Phys. Rev. Lett. 134 (2025) 121902.

Parameter Values and Uncertainties

Parameter	Value	Parameter	Value
N_u	$0.0223^{+0.0029}_{-0.0024}$	$N_{\bar{u}}$	$-0.008^{+0.092}_{-0.035}$
N_d	$0.0353^{+0.0051}_{-0.0088}$	$N_{\bar{d}}$	$0.006^{+0.032}_{-0.011}$
N_s	$-0.022^{+0.043}_{-0.043}$	N_g	$0.0220^{+0.0081}_{-0.0706}$
α_u	$2.78^{+0.45}_{-0.72}$	α_d	$4.28^{+0.38}_{-0.76}$
β_u	$0.145^{+0.041}_{-0.194}$	β_d	$1.16^{+0.14}_{-0.40}$
ϵ_u	$7.4^{+2.3}_{-4.5}$	ϵ_d	$-0.59^{+0.18}_{-0.20}$
λ_1	$0.240^{+0.062}_{-0.134}$	λ_2	$0.39^{+0.13}_{-0.33}$
λ_3	$0.92^{+12.17}_{-0.92}$	λ_4	$7.50^{+2.29}_{-0.78}$
λ_5	$-1.11^{+0.87}_{-0.50}$		

K. Yang, TL, P. Sun, Y. Zhao, B.-Q. Ma, Phys. Rev. Lett. 134 (2025) 121902.

Correlation Matrix of the Parameters

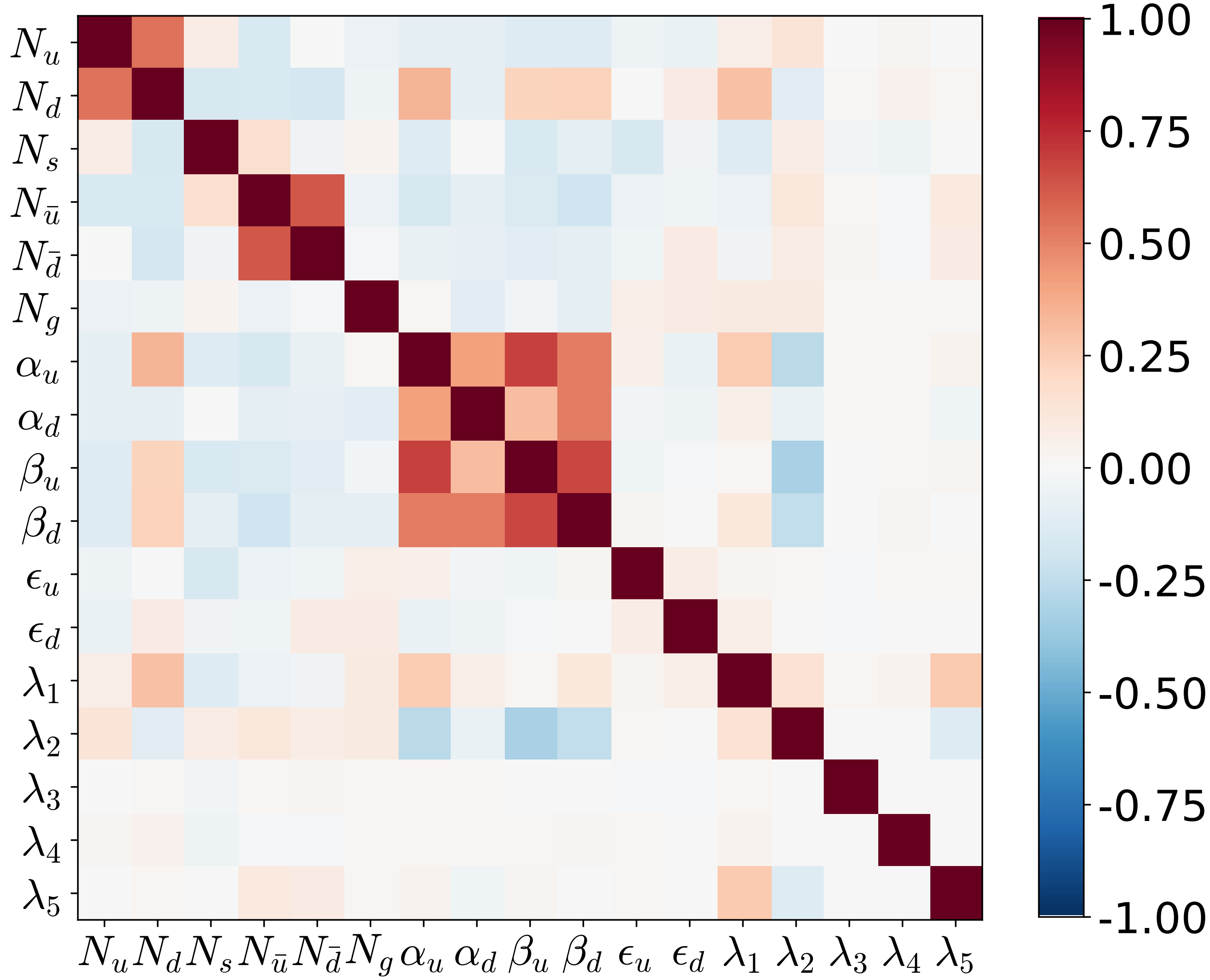

K. Yang, TL, P. Sun, Y. Zhao, B.-Q. Ma, Phys. Rev. Lett. 134 (2025) 121902.

Comparison with Data

Compare with HERMES data

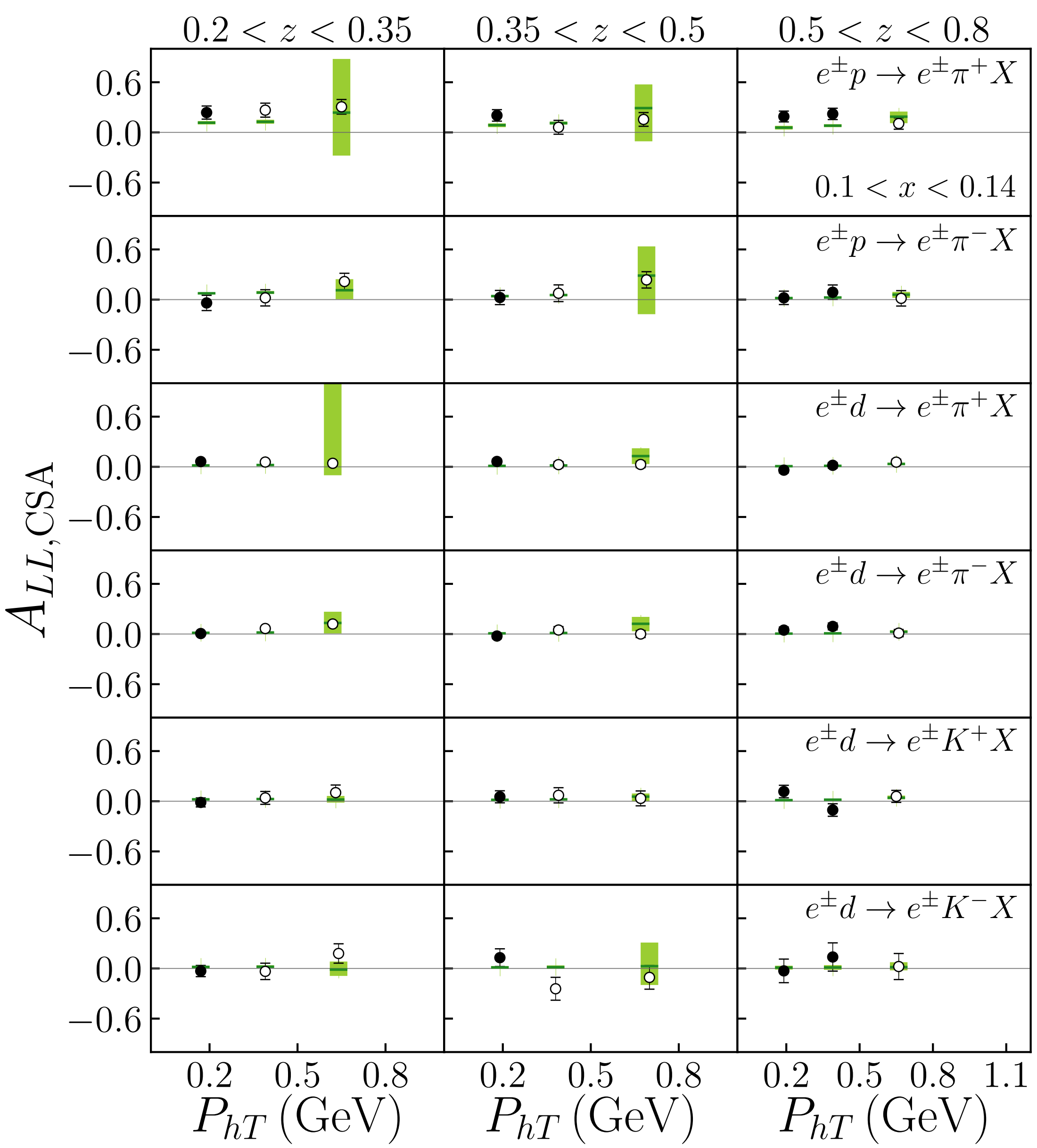

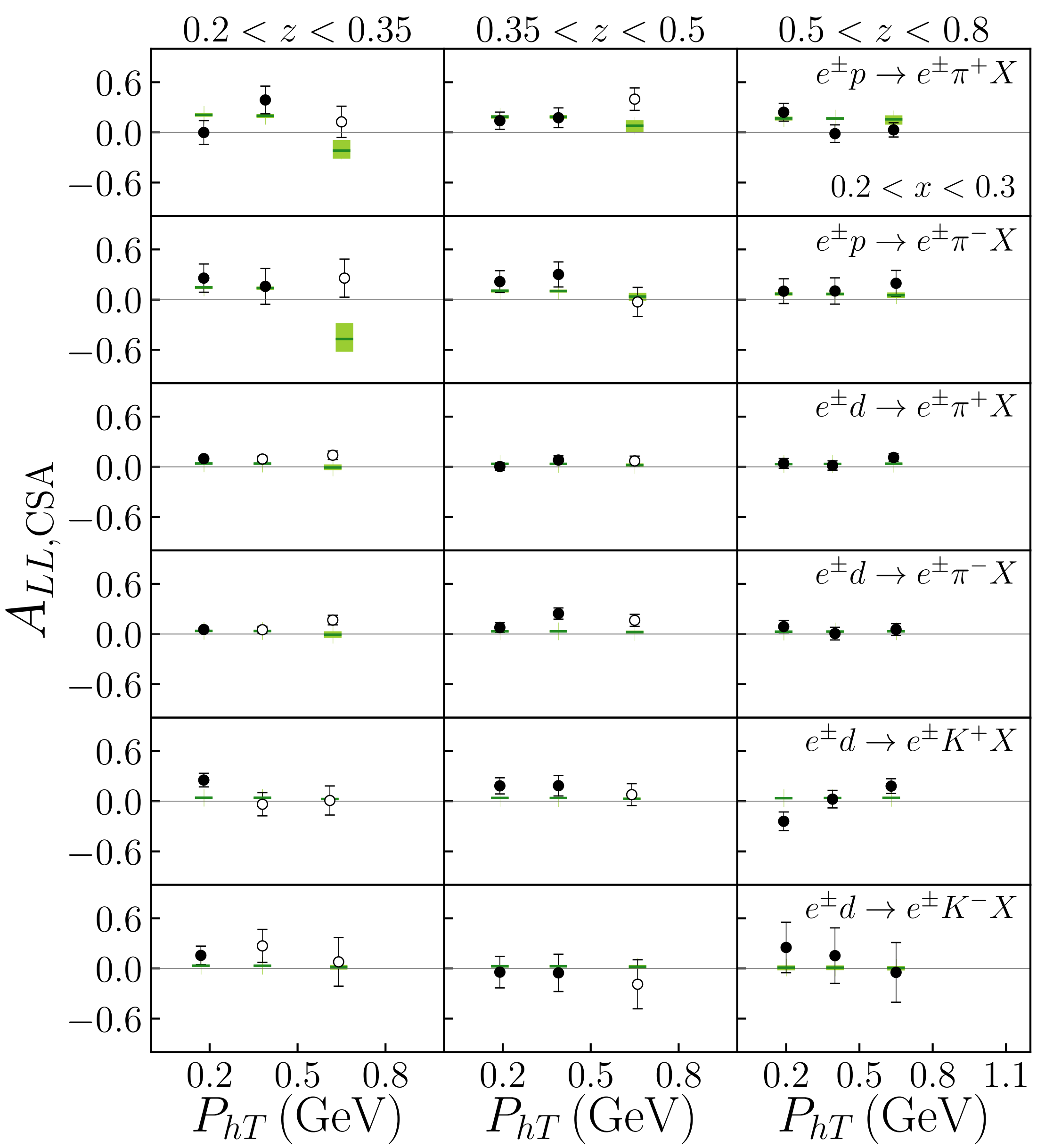

K. Yang, TL, P. Sun, Y. Zhao, B.-Q. Ma, Phys. Rev. Lett. 134 (2025) 121902.

Comparison with Data

Compare with HERMES data

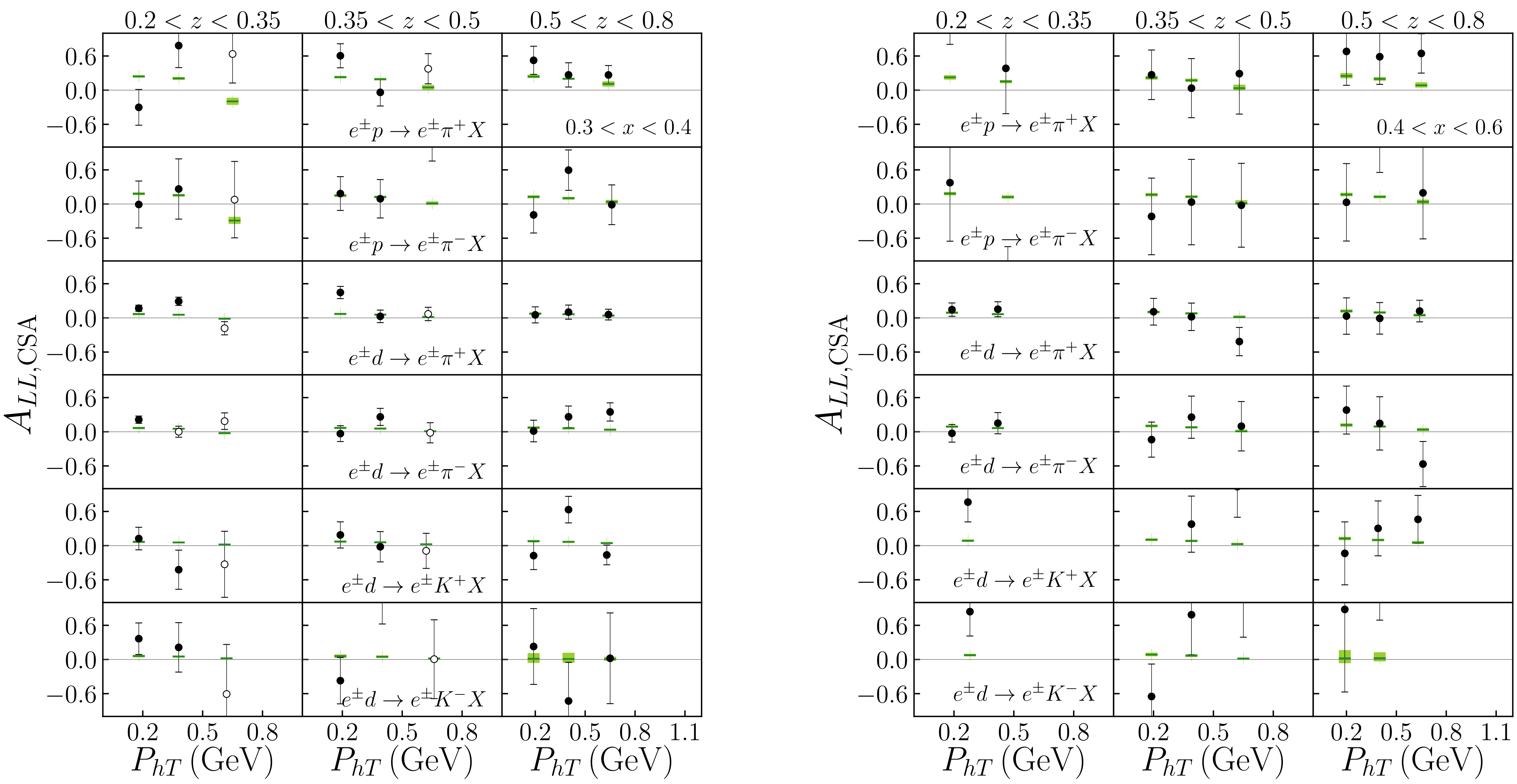

K. Yang, TL, P. Sun, Y. Zhao, B.-Q. Ma, Phys. Rev. Lett. 134 (2025) 121902.

Comparison with Data

Compare with HERMES data

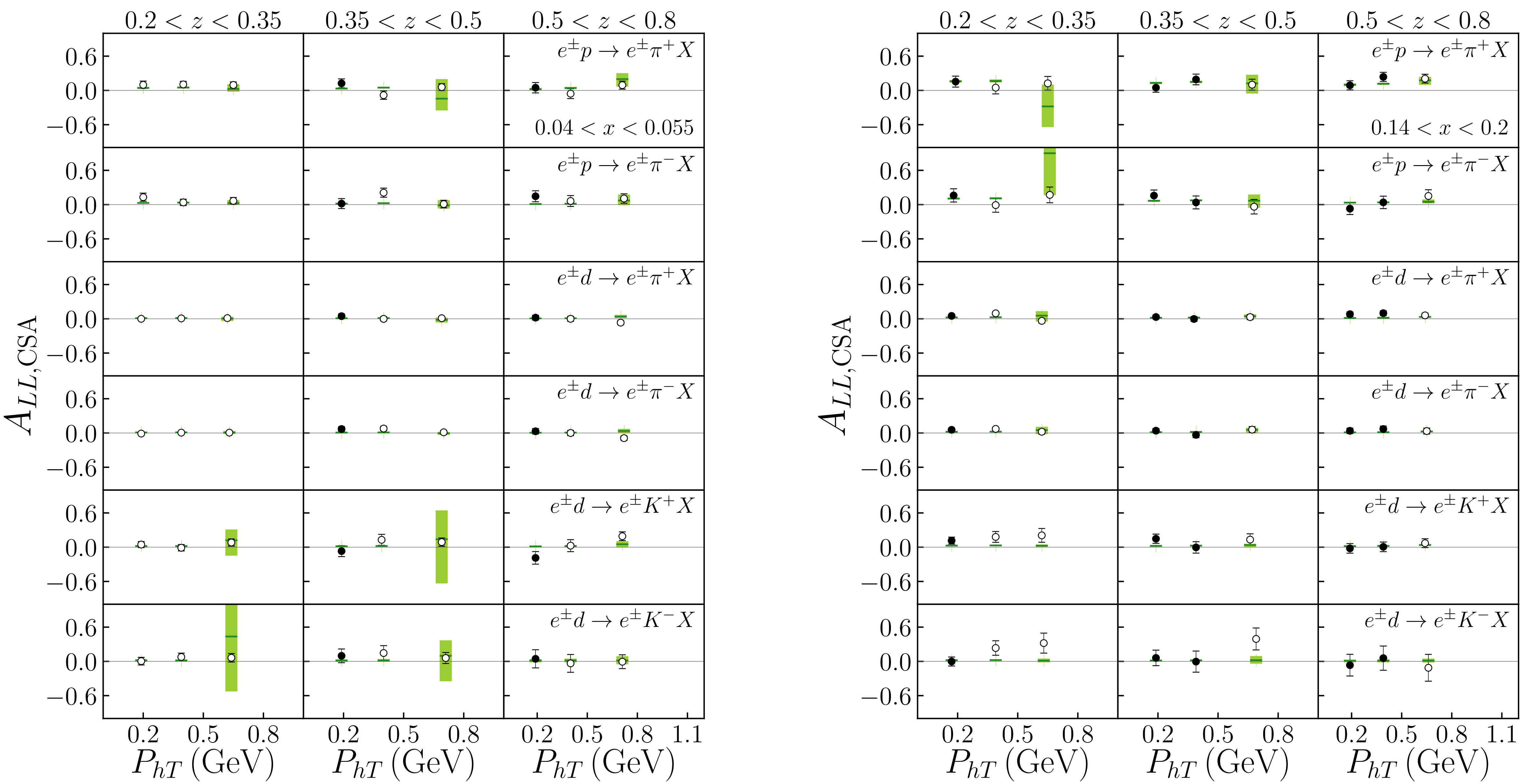

K. Yang, TL, P. Sun, Y. Zhao, B.-Q. Ma, Phys. Rev. Lett. 134 (2025) 121902.

Comparison with Data

Compare with HERMES data

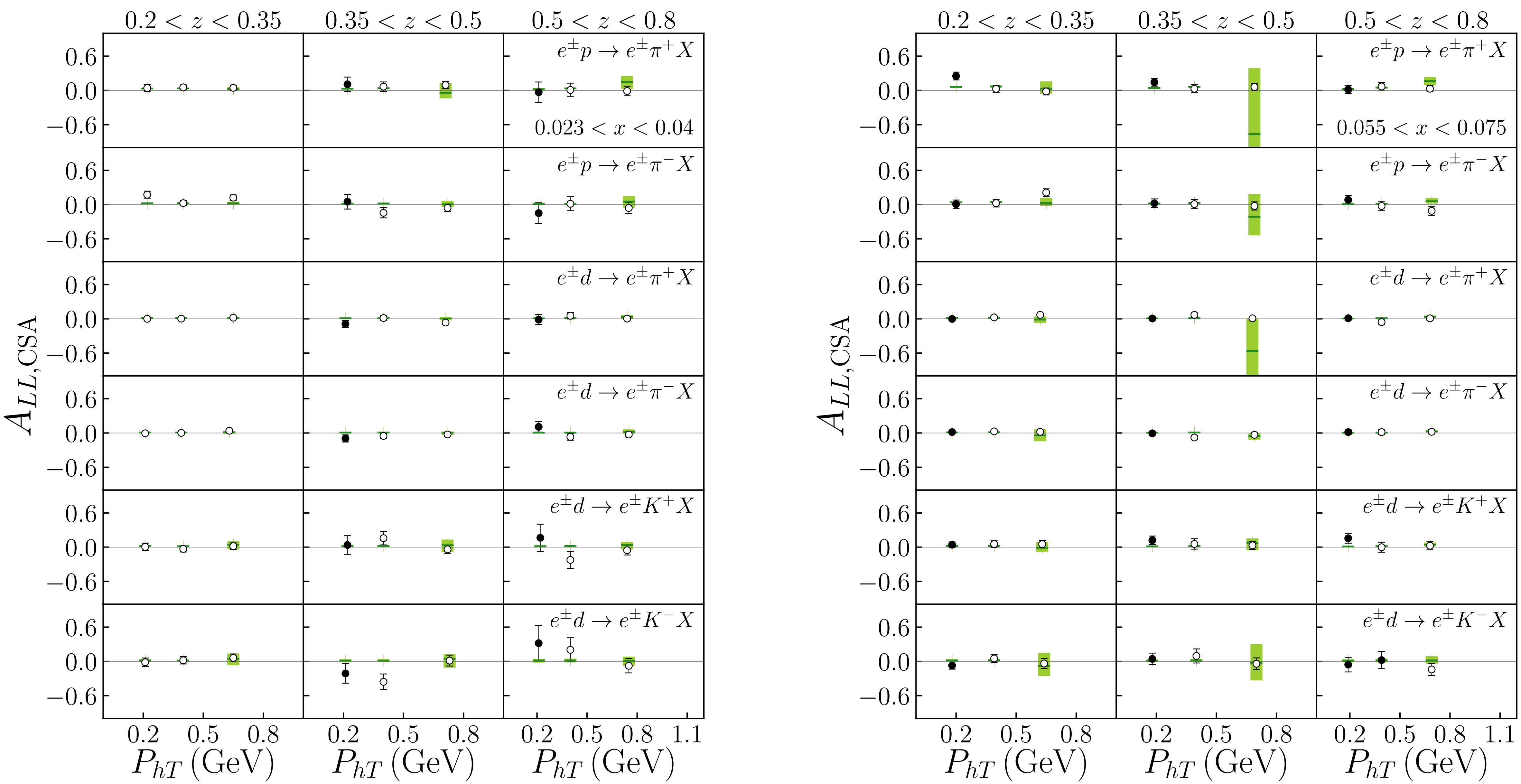

K. Yang, TL, P. Sun, Y. Zhao, B.-Q. Ma, Phys. Rev. Lett. 134 (2025) 121902.

Comparison with Data

Compare with HERMES data

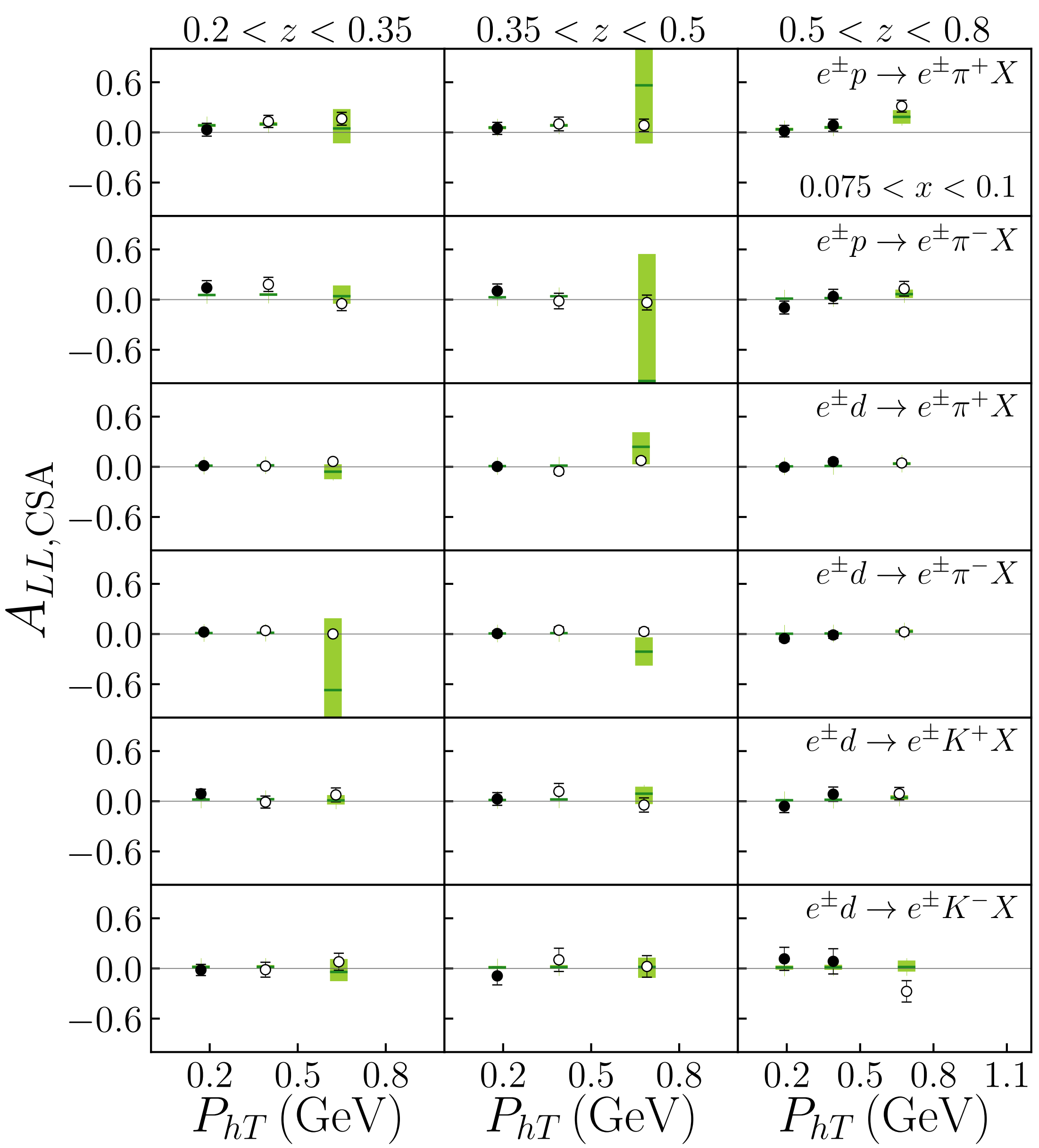

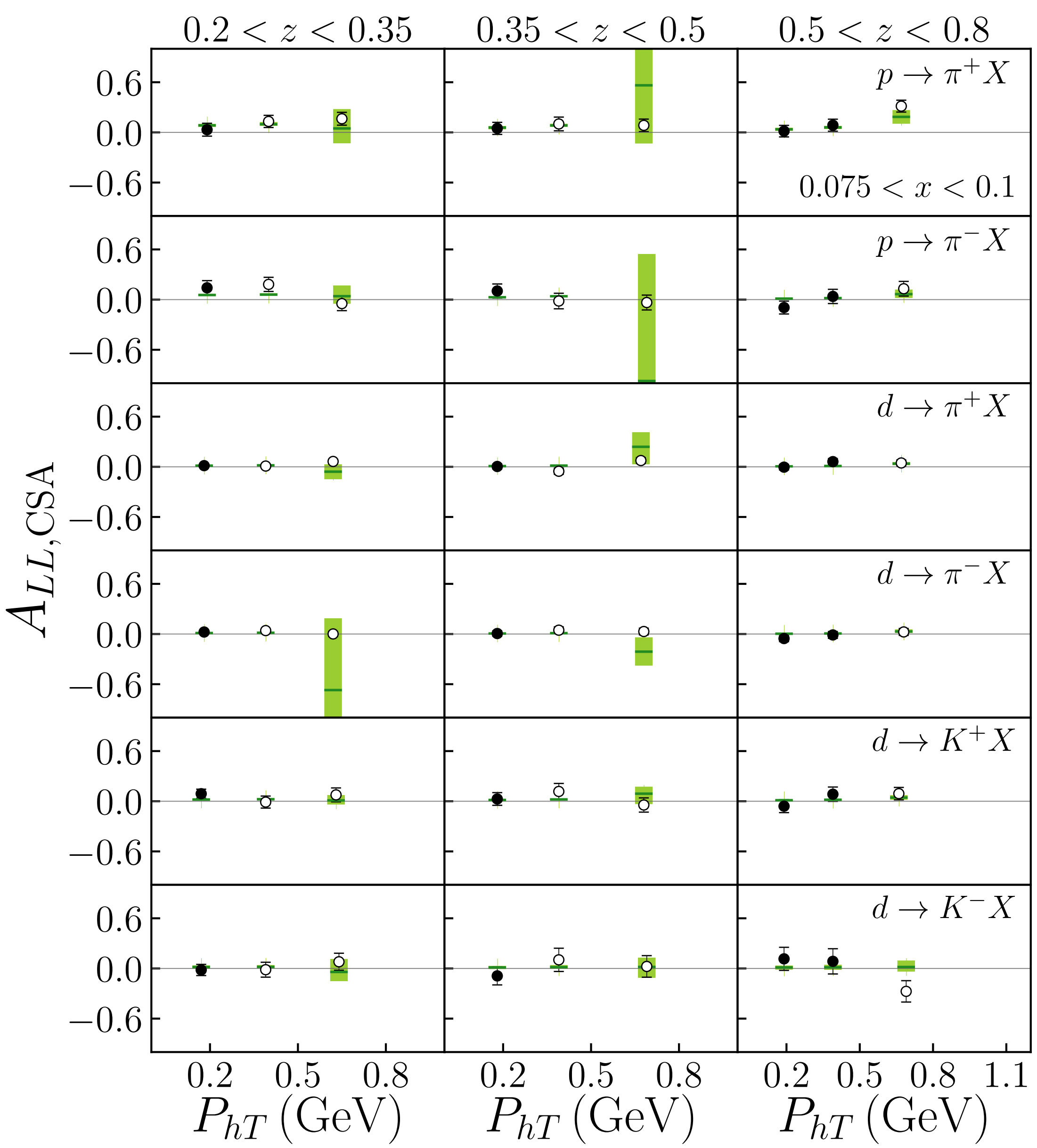

K. Yang, TL, P. Sun, Y. Zhao, B.-Q. Ma, Phys. Rev. Lett. 134 (2025) 121902.

Comparison with Data

Compare with CLAS data

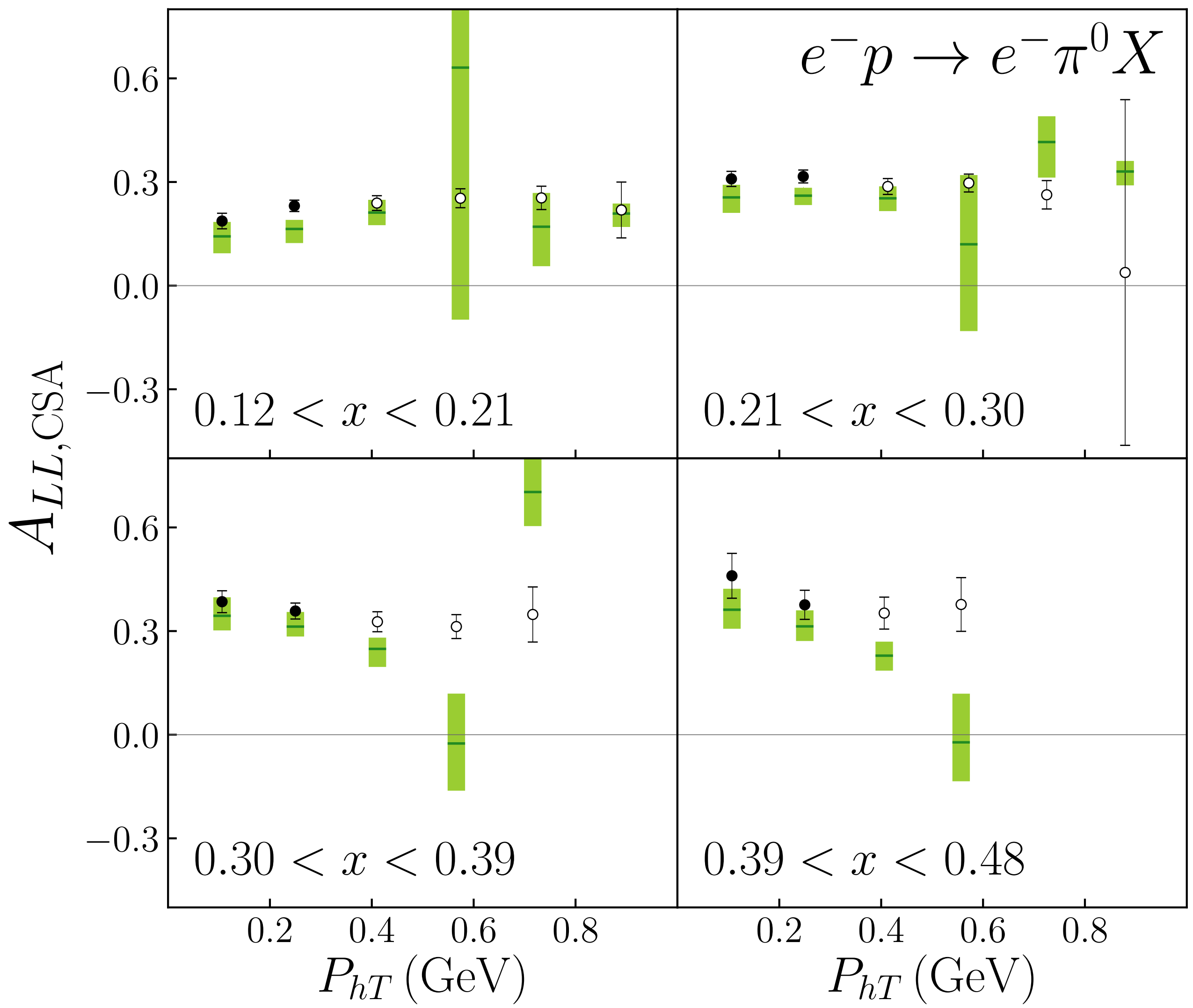

K. Yang, TL, P. Sun, Y. Zhao, B.-Q. Ma, Phys. Rev. Lett. 134 (2025) 121902.

Transverse Momentum Dependent Polarization

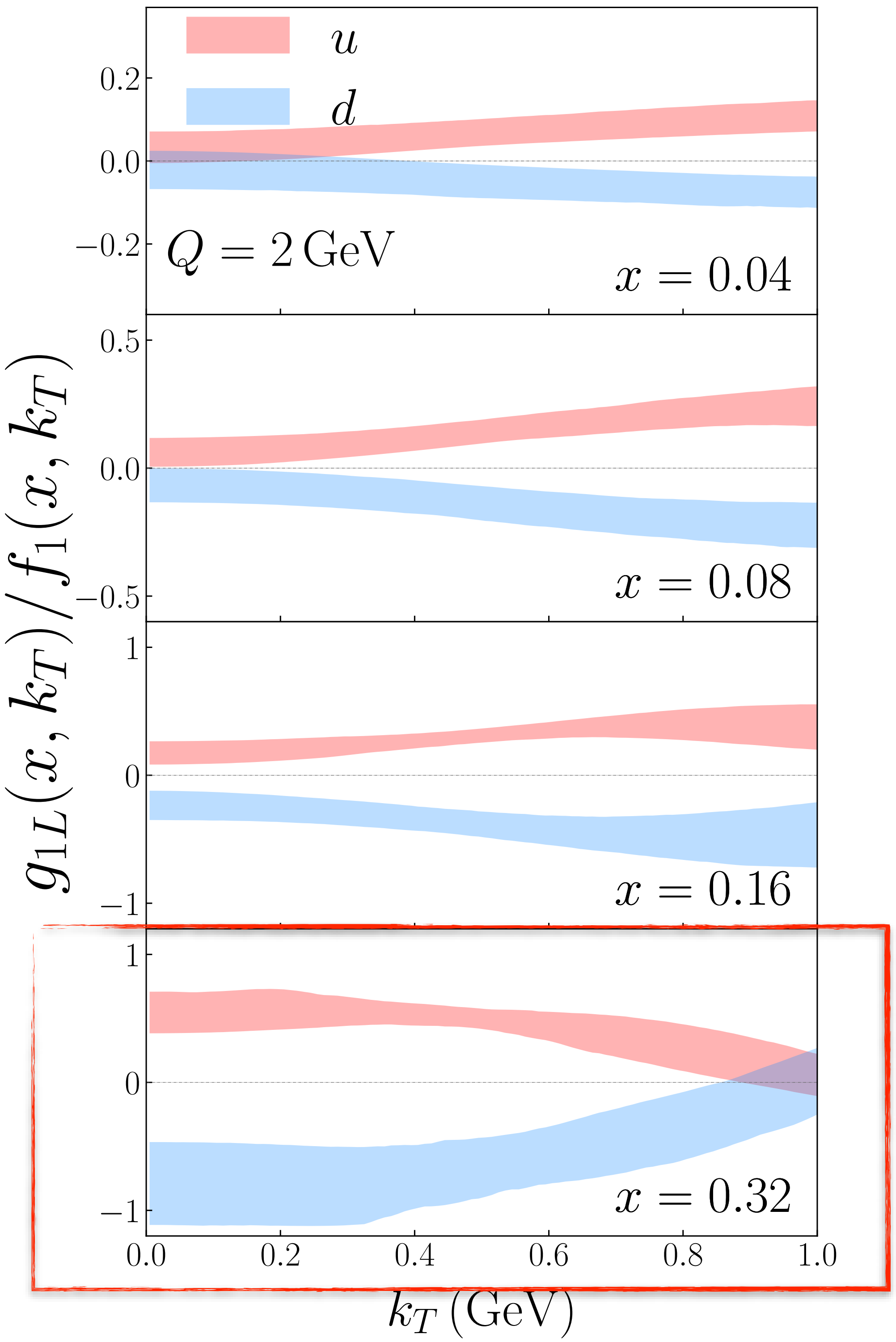

$g_{1L}(x, k_T^2) = q_\uparrow(x, k_T^2) - q_\downarrow(x, k_T^2)$
measures the absolute number density difference between spin-parallel and spin-antiparallel quarks in a polarized proton.

$$\frac{g_{1L}(x, k_T^2)}{f_1(x, k_T^2)} = \frac{q_\uparrow(x, k_T^2) - q_\downarrow(x, k_T^2)}{q_\uparrow(x, k_T^2) + q_\downarrow(x, k_T^2)}$$

measures the polarization rate of quarks.

- At large x, where valence components dominate, the polarization decreases with increasing k_T
  Qualitatively consistent with kinetic Wigner rotation effects

K. Yang, TL, P. Sun, Y. Zhao, B.-Q. Ma, Phys. Rev. Lett. 134 (2025) 121902.

Transverse Momentum Dependent Polarization

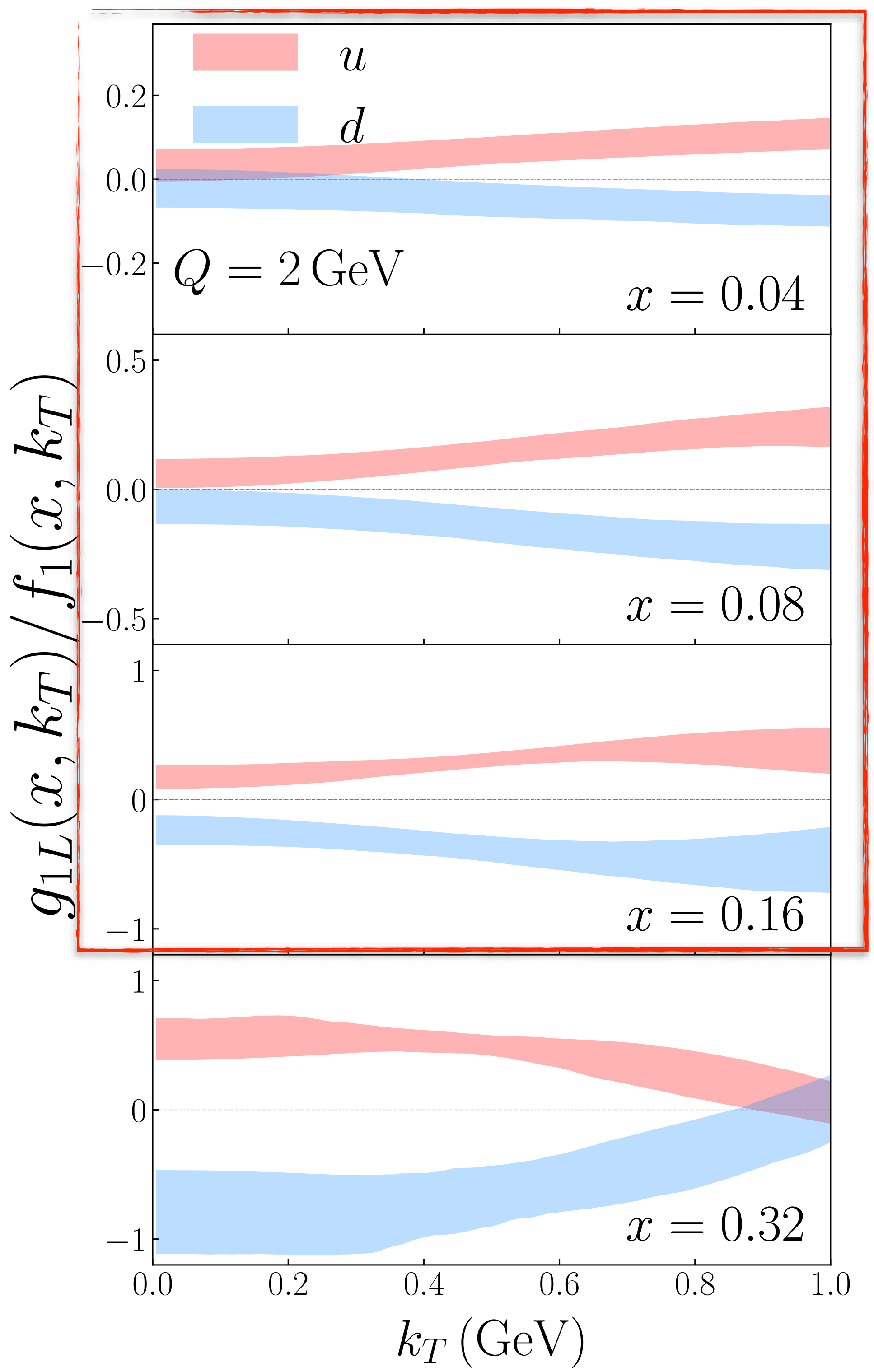

$g_{1L}(x, k_T^2) = q_\uparrow(x, k_T^2) - q_\downarrow(x, k_T^2)$
measures the absolute number density difference between spin-parallel and spin-antiparallel quarks in a polarized proton.

$$\frac{g_{1L}(x, k_T^2)}{f_1(x, k_T^2)} = \frac{q_\uparrow(x, k_T^2) - q_\downarrow(x, k_T^2)}{q_\uparrow(x, k_T^2) + q_\downarrow(x, k_T^2)}$$

measures the polarization rate of quarks.

- At low x, where the valence component is no longer adequate, distributions are highly driven by complex QCD dynamics
  The polarization is found increasing with k_T

K. Yang, TL, P. Sun, Y. Zhao, B.-Q. Ma, Phys. Rev. Lett. 134 (2025) 121902.

Examine the Positivity Bound

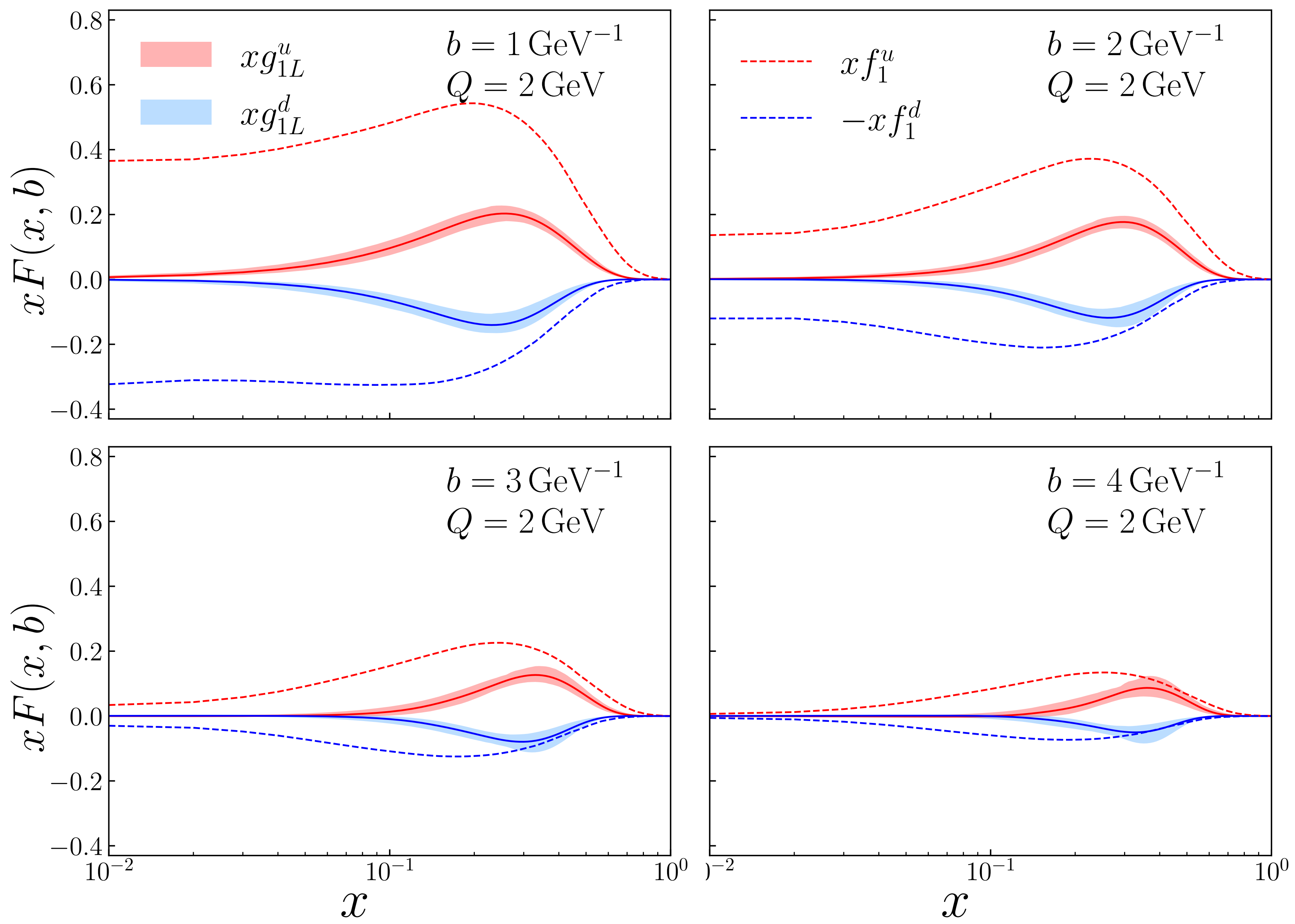

Positivity bound: $|g_{1L}| \leq f_1$
based on probability interpretation

It *should not* be imposed during the fit, which will introduce bias to results.

It can be examined.
No breaking of the bound is observed according to current uncertainties.

K. Yang, TL, P. Sun, Y. Zhao, B.-Q. Ma, Phys. Rev. Lett. 134 (2025) 121902.

Test the Sensitivity to FFs

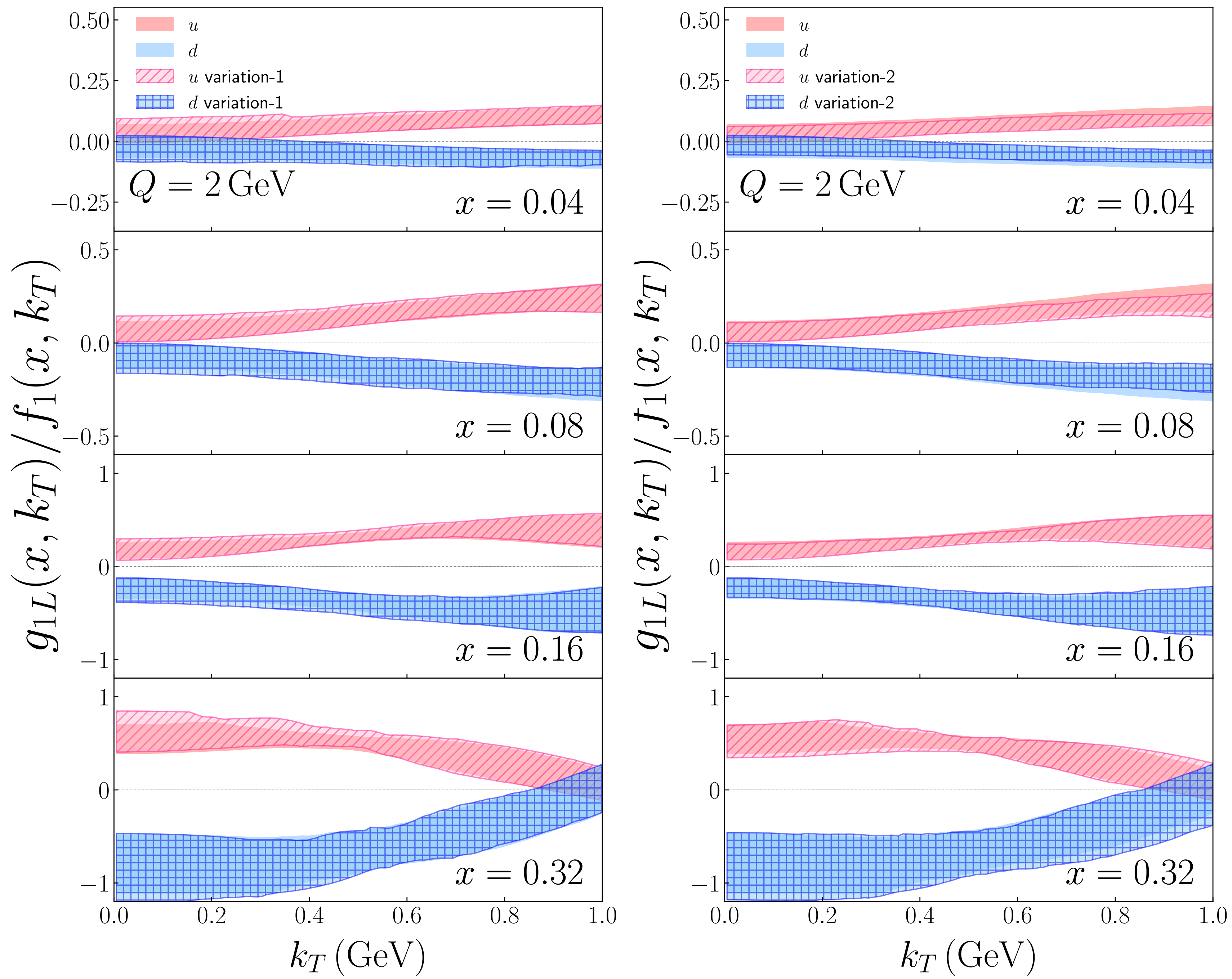

Input of TMD FFs: $D_1(z, p_T^2)$
SV19-DSS parametrization

The polarization distributions, i.e. the ratio between g_{1L} and f_1, are not sensitive to the choice of input FFs.

K. Yang, TL, P. Sun, Y. Zhao, B.-Q. Ma, Phys. Rev. Lett. 134 (2025) 121902.

Flexible vs. Fixed x-dependence

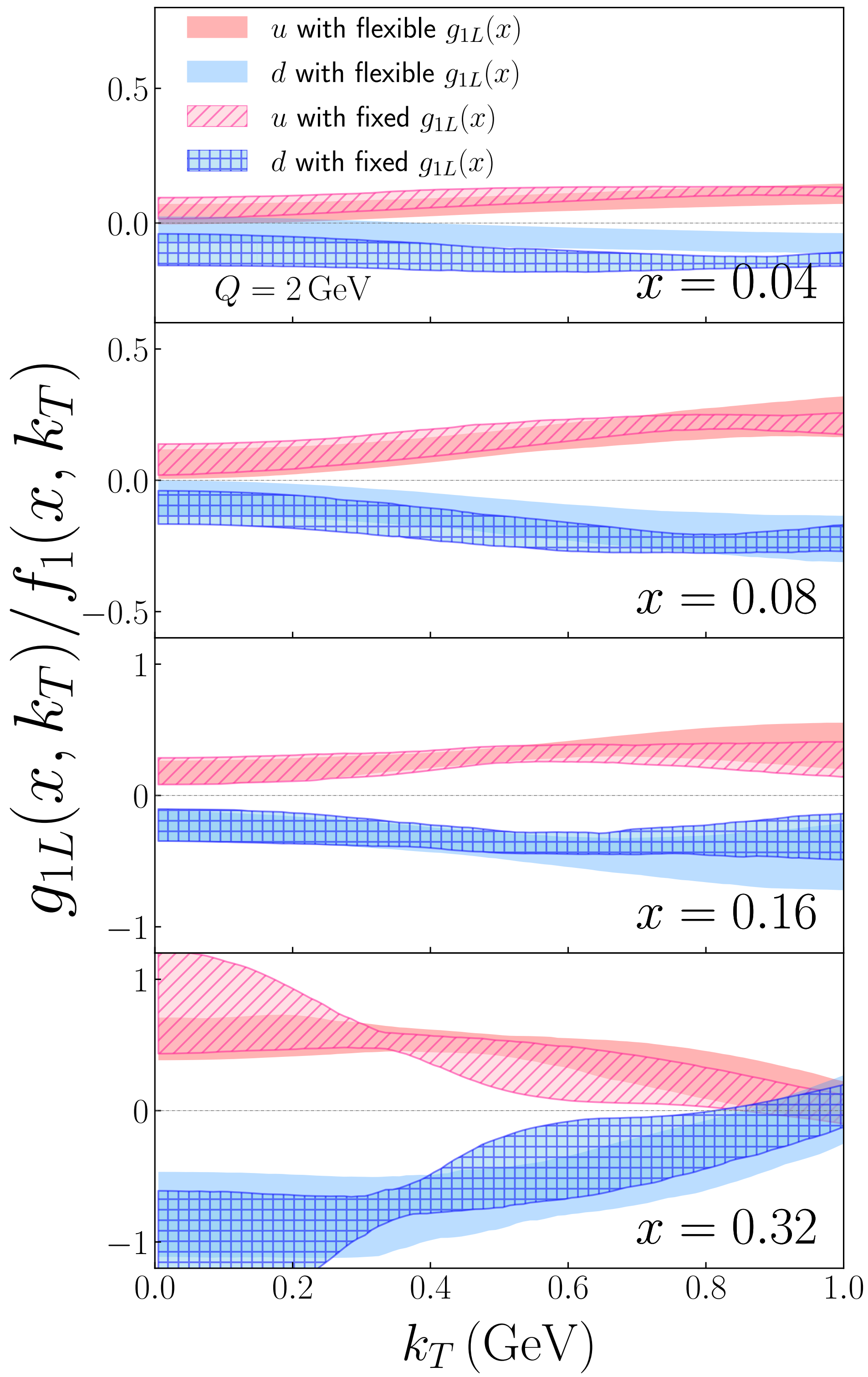

Recall the parametrization:

$$g_{1L}^f(x) = N_f \frac{(1-x)^{\alpha_f} x^{\beta_f}\left(1+\epsilon_f x\right)}{n\left(\alpha_f, \beta_f, \epsilon_f\right)} g_1^f\left(x, \mu_{\mathrm{OPE}}\right)$$

By setting $\alpha_f = \beta_f = \epsilon_f = 0$, one can fix it to the collinear distributions.

The results from these two choices are consistent within current uncertainties.

K. Yang, TL, P. Sun, Y. Zhao, B.-Q. Ma, Phys. Rev. Lett. 134 (2025) 121902.

Further Exploration of Azimuthal Modulation

Comparison between theoretical calculations and HERMES data

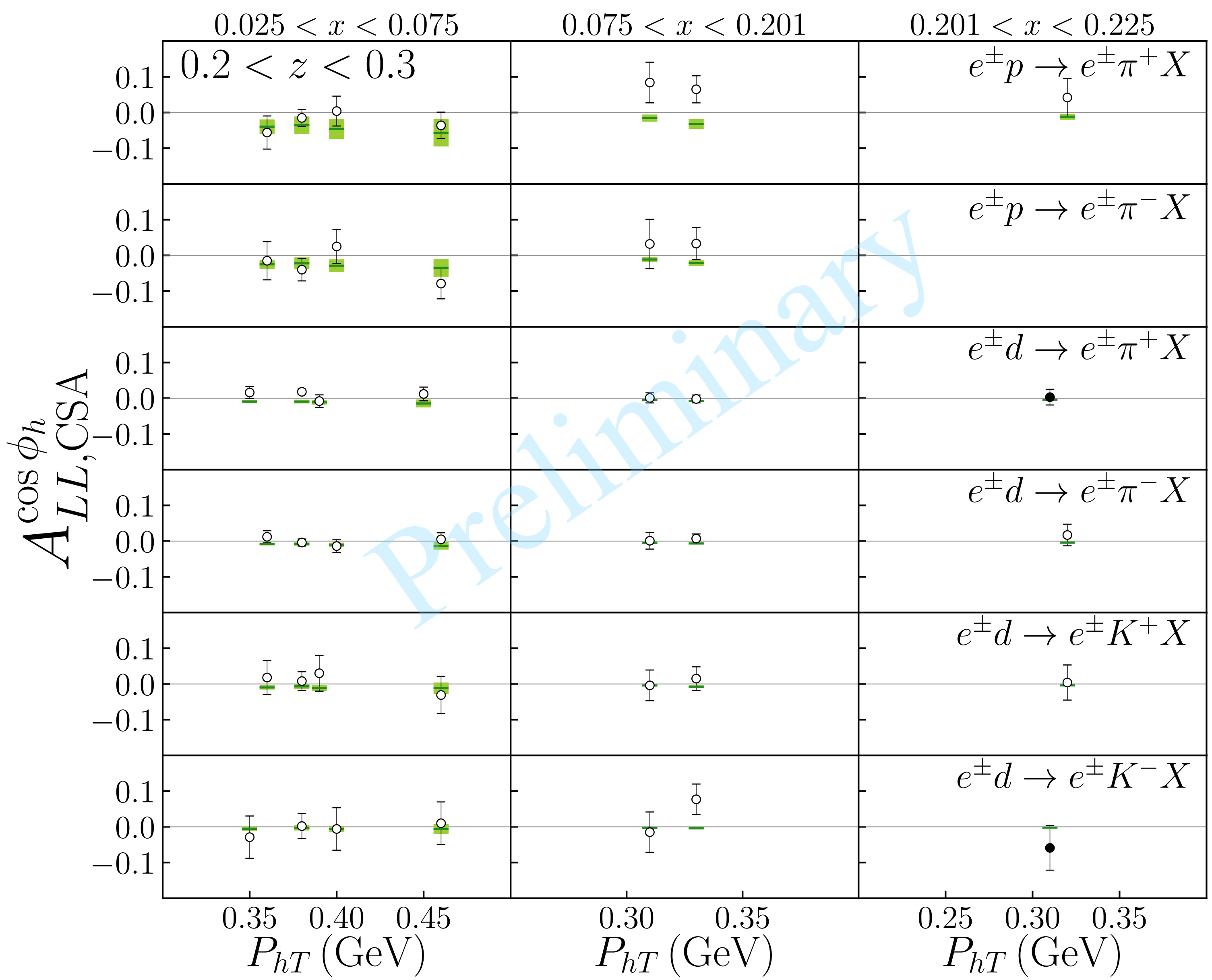

Further Exploration of Azimuthal Modulation

Comparison between theoretical calculations and HERMES data

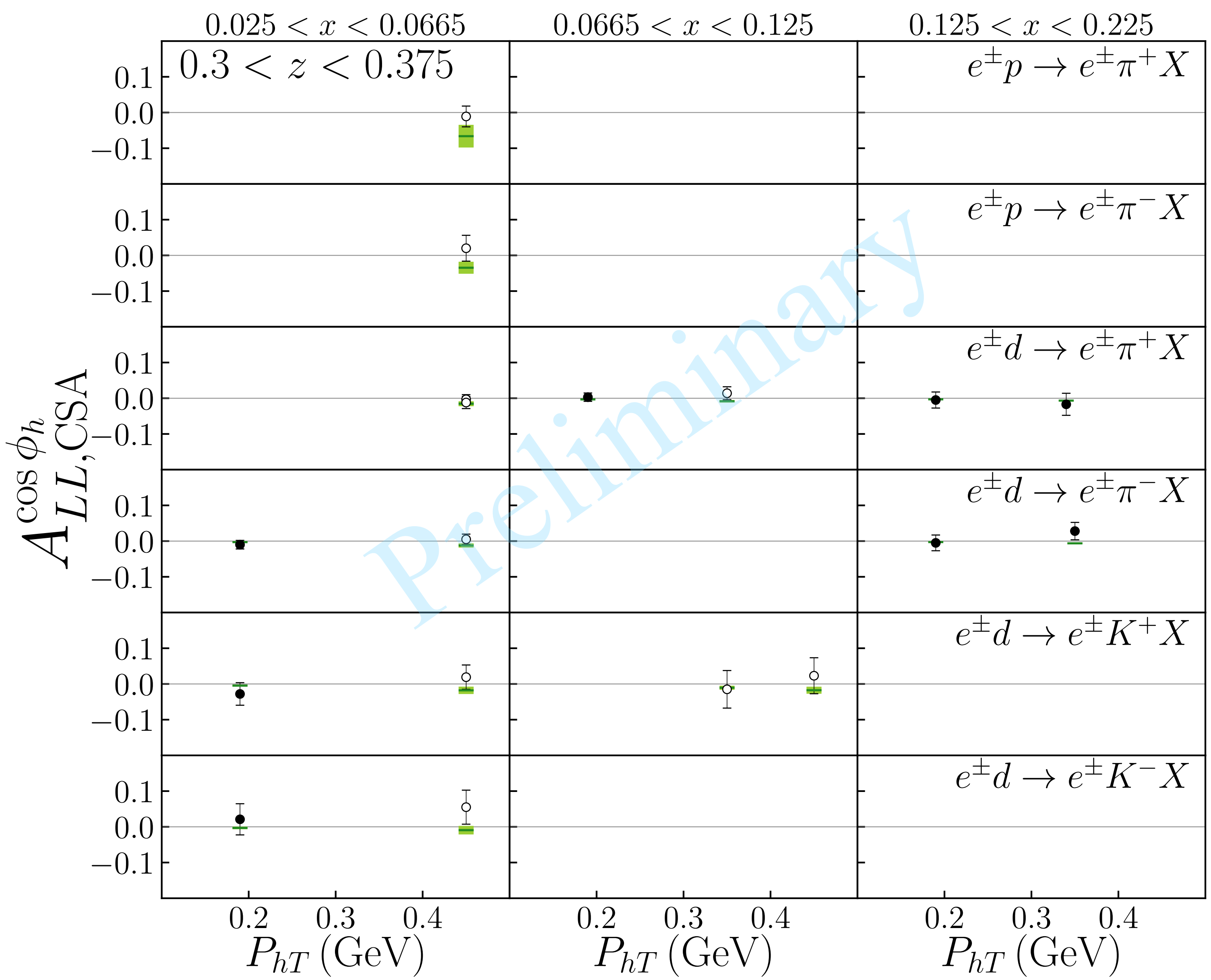

Further Exploration of Azimuthal Modulation

Comparison between theoretical calculations and HERMES data

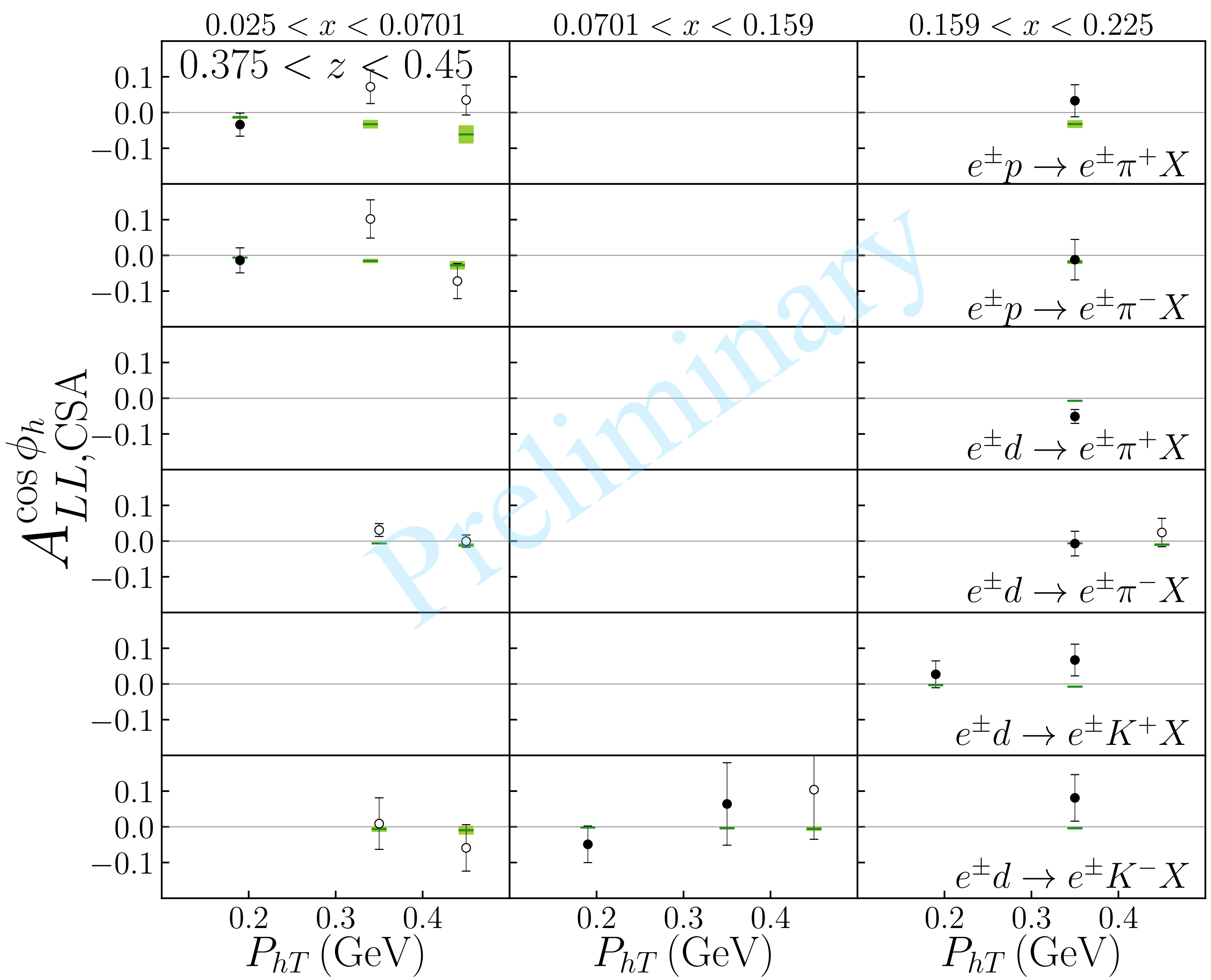

Further Exploration of Azimuthal Modulation

Comparison between theoretical calculations and HERMES data

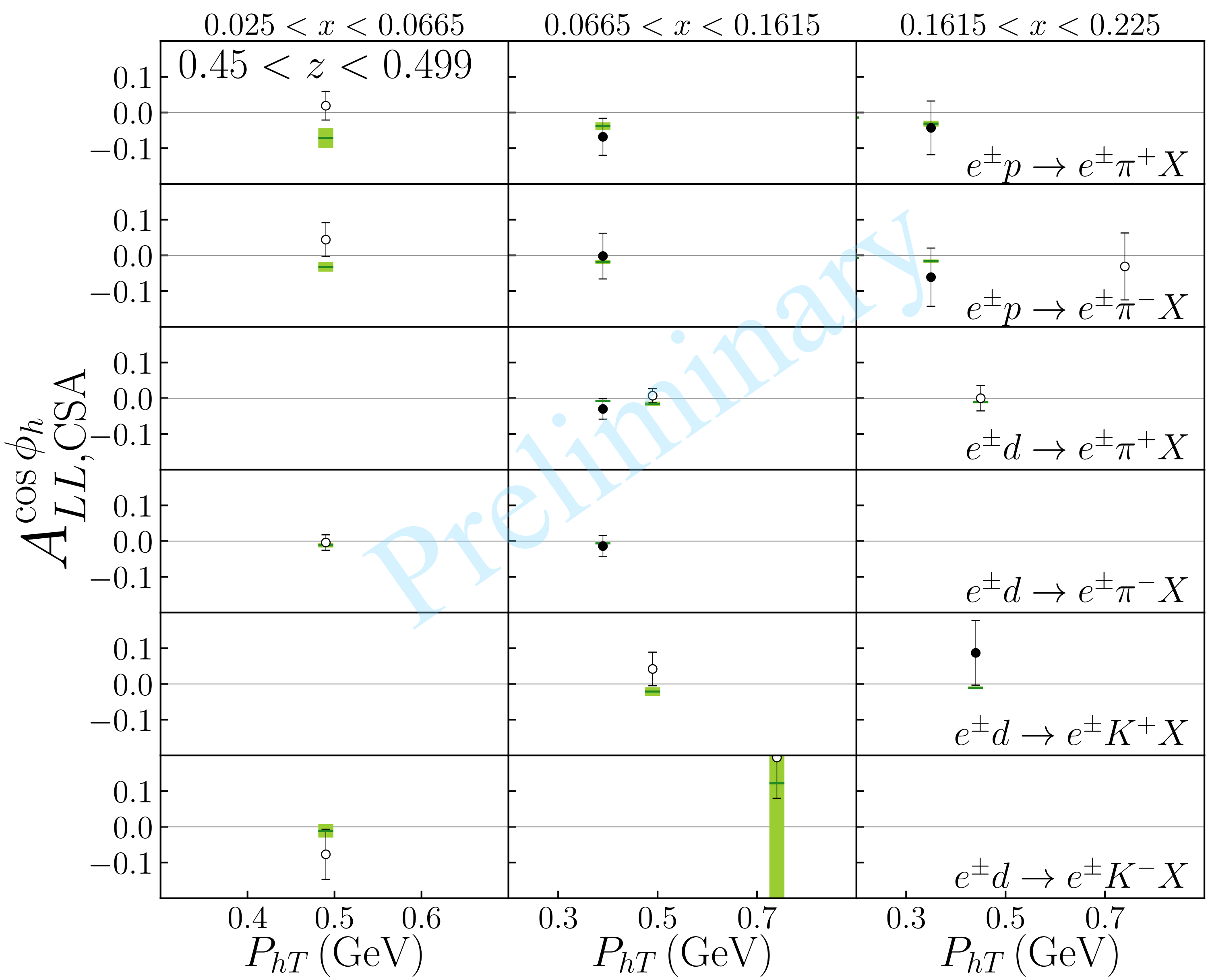

SHANDONG UNIVERSITY, QINGDAO

Further Exploration of Azimuthal Modulation

Comparison between theoretical calculations and HERMES data

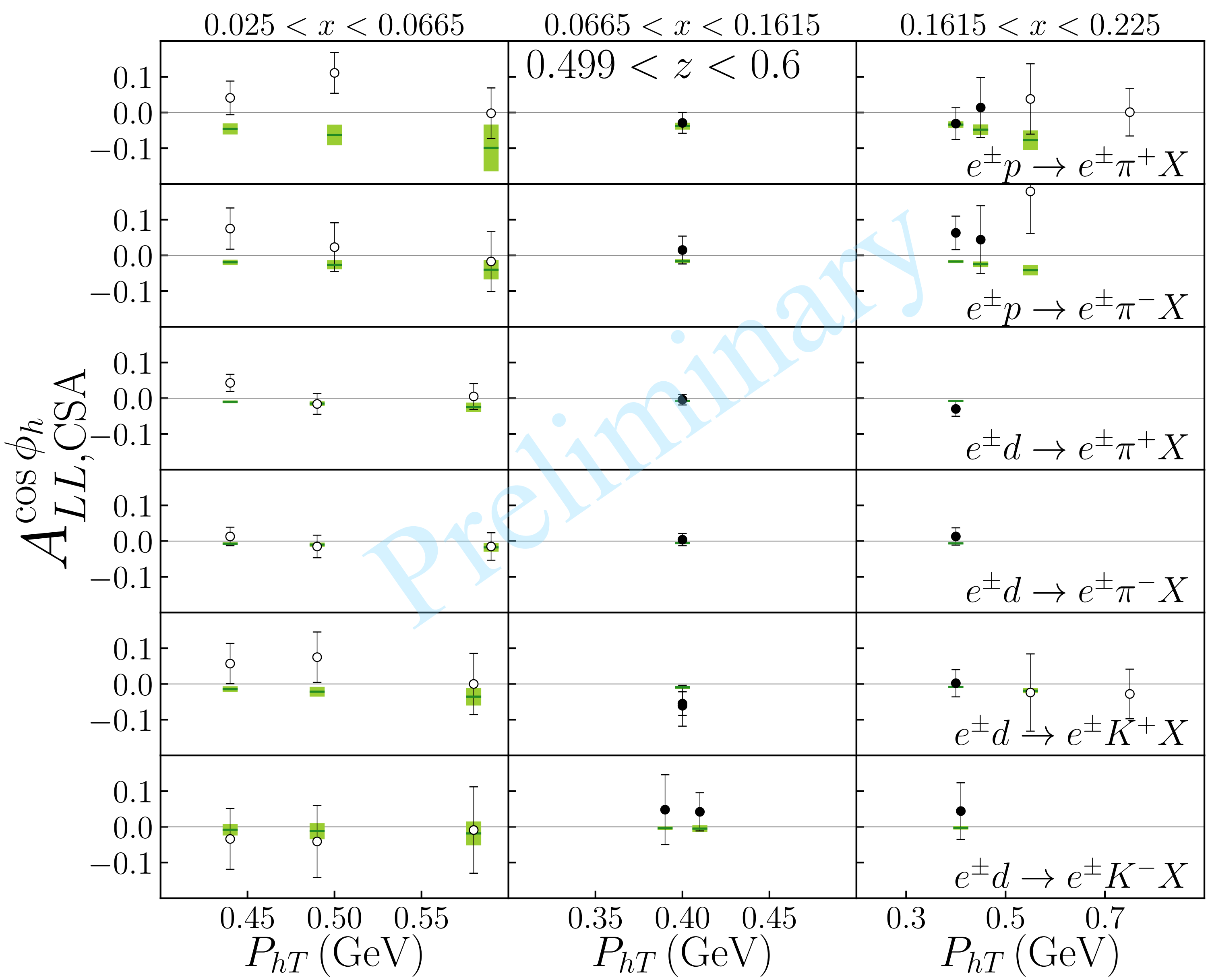

Further Exploration of Azimuthal Modulation

Comparison between theoretical calculations and HERMES data

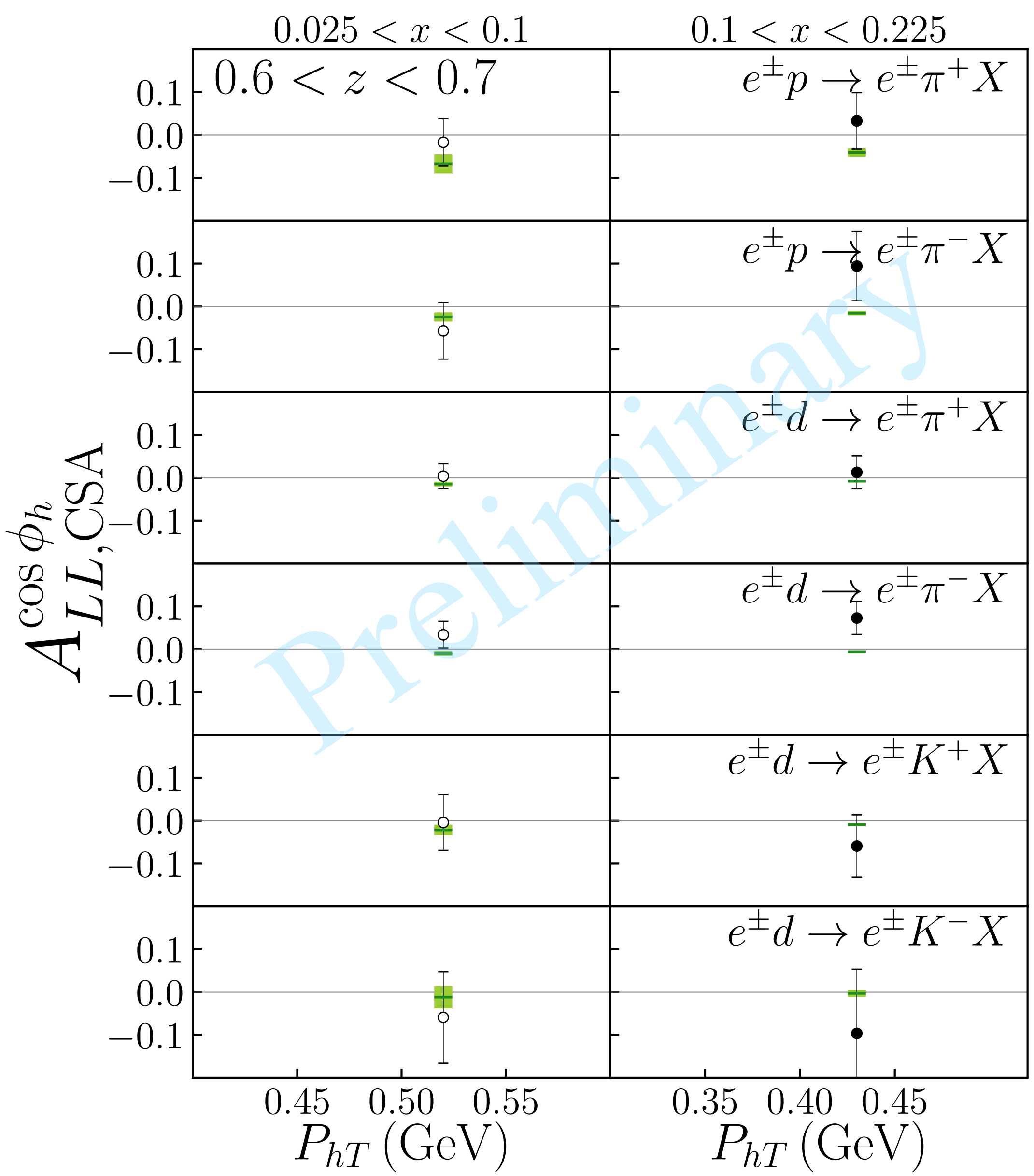

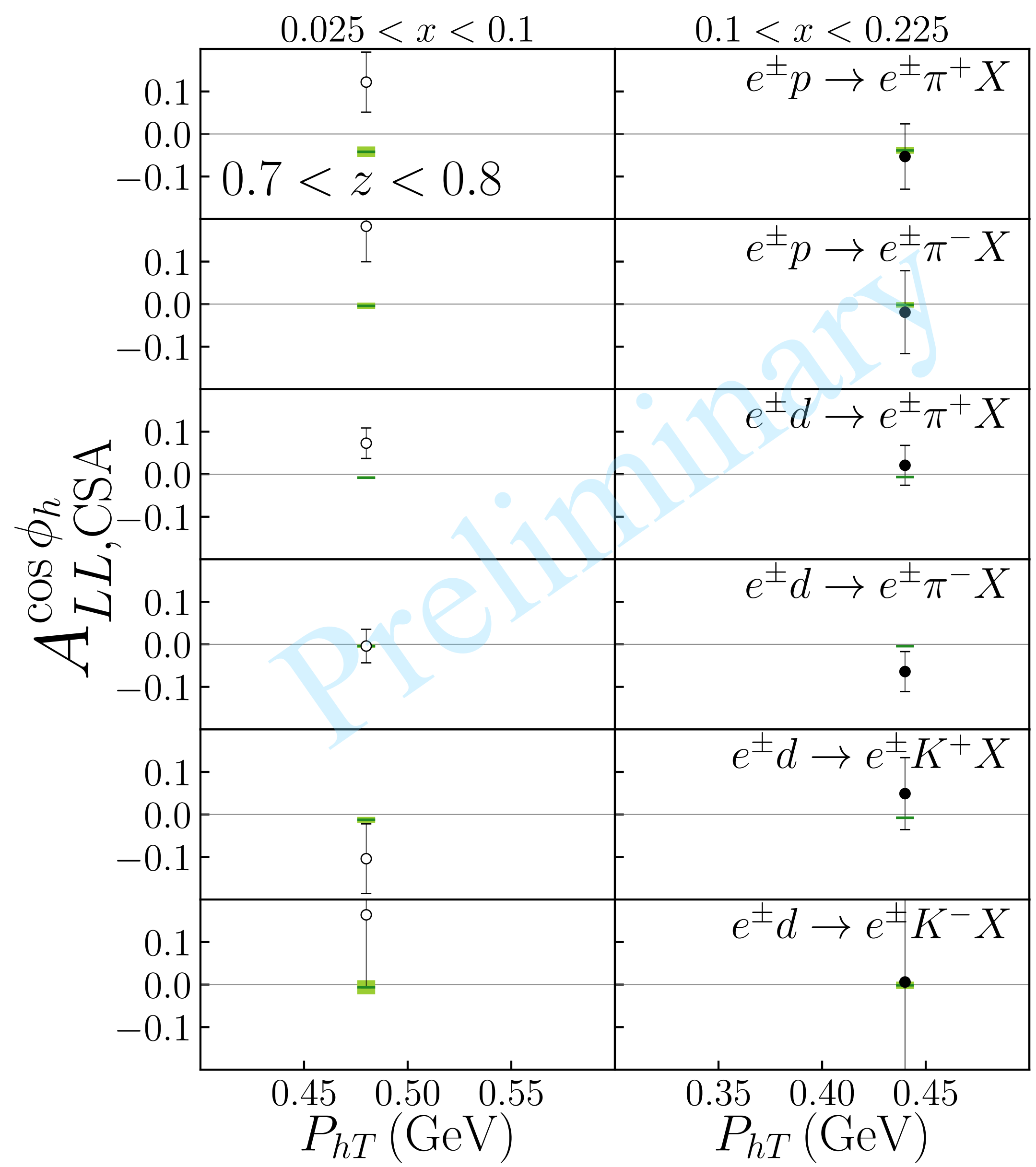

Further Exploration of Azimuthal Modulation

Comparison between theoretical calculations and CLAS data

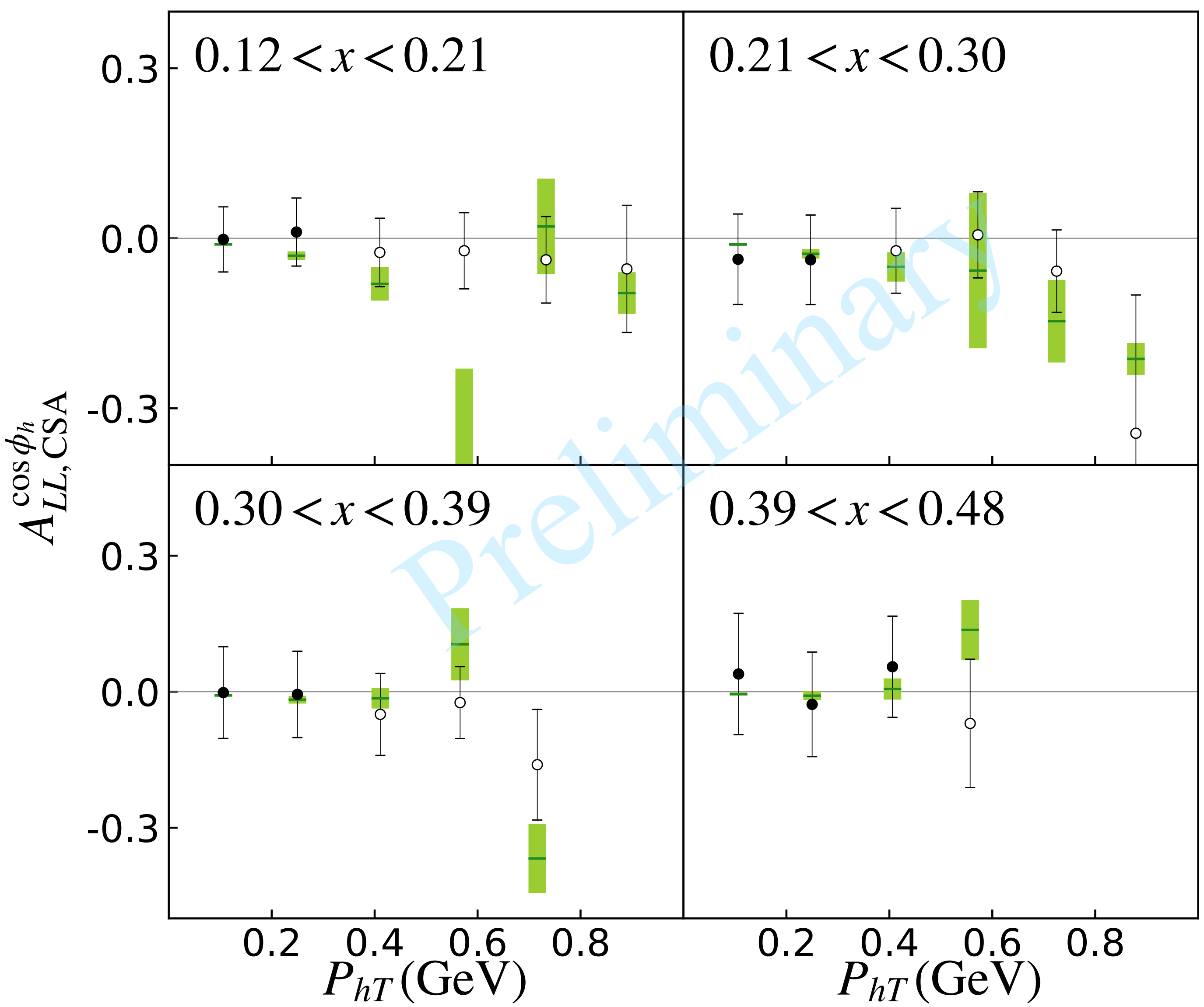

Transverse Nucleon Tomography Collaboration

Tianbo Liu
SDU

Bo-Qiang Ma
PKU/ZZU

Peng Sun
IMP

Yuxiang Zhao
IMP

Hongxin Dong
NJNU

Ke Yang
PKU

Chunhua Zeng
LZU

Transverse Nucleon Tomography Collaboration

Sivers distribution functions:

Chunhua Zeng, Tianbo Liu, Peng Sun, Yuxiang Zhao, Phys. Rev. D 106 (2022) 094039.

Transversity distribution functions and Collins fragmentation functions:

Chunhua Zeng, Hongxin Dong, Tianbo Liu, Peng Sun, Yuxiang Zhao, Phys. Rev. D 109 (2024) 056002.

Trans-helicity worm-gear distribution functions:

Ke Yang, Tianbo Liu, Peng Sun, Yuxiang Zhao, Bo-Qiang Ma, Phys. Rev. D 110 (2024) 034036.

Transverse momentum dependent helicity distribution functions:

Ke Yang, Tianbo Liu, Peng Sun, Yuxiang Zhao, Bo-Qiang Ma, Phys. Rev. Lett. 134 (2025) 121902.

Sivers, transversity, and Collins functions including DY and new COMPASS data:

Chunhua Zeng, Hongxin Dong, Tianbo Liu, Peng Sun, Yuxiang Zhao, Phys. Lett. B (2025).

Helicity distributions and azimuthal modulations in longitudinal DSA:

Ke Yang, Tianbo Liu, Peng Sun, Yuxiang Zhao, Bo-Qiang Ma, in preparation.

Summary and Outlook

- Spin always surprises since its discovery 100 years ago
- Nucleon spin structure is still not well understood
- Rich information is contained in multidimensional imagings, TMDs as well as GPDs
- First extraction of TMD helicity distributions is obtained by analyzing transverse momentum dependent SIDIS DSA data

  - at large-x region, where valence components dominate, quark polarization decreases with increasing k_T, supporting the kinetic Wigner rotation effects;

  - in low-x region, increasing quark polarization in dependence on k_T is observed, indicating the essential role of QCD dynamics;

  - sea quarks and gluon distributions are loosely constrained by existing SIDIS data.

- Transverse momentum dependent measurements of W production in polarized pp collisions at RHIC may help constrain sea quark distributions.
- Opportunities from existing experiments at RHIC, JLab12, BESIII, BelleII, and future facilities, EIC, EicC, STCF, to understand nucleon spin structures and fragmentation functions.

Thank you!